POLITECNICO DI TORINO

Master's Degree in Environmental and Land Engineering

Evaluation of MODIS products for the quantification of crop water stress in Piedmont

Supervisors
Prof. Stefania Tamea
Ing. Matteo Rolle

Candidate
Margherita Urbini

Academic Year 2022-2023

A mia nonna Argentina

Abstract

Drought periods are increasing their frequency as consequence of climate change and the agricultural sector is one of the most affected due to the water demand and growing request of agricultural commodities. Thus, water management for a sustainable agriculture is becoming challenging. In this context, the need to estimate soil evapotranspiration (ET) arises because it is critical for crop water stress assessment as well as hydrological modelling, irrigation scheduling, water management and weather forecasting. Since an accurate estimation of ET is difficult to reach across different spatial and temporal scales, a satellite-based product for this type of analysis proves to be very useful. The purpose of this study is to analyse the water stress in the Piedmont region in Italy, which in recent years has been increasingly affected by intense periods of drought, to which it is not usually subject. In addition, the study aims at comparing the performance of the satellite-based MODIS evapotranspiration operational product (M*D16A2) with a mathematical soil water balance model. This latter provides an estimation of crop evapotranspiration based on the Food and Agriculture Organization guidelines (FAO n.56). The time frame of the analysis includes the two-year period 2021-2022, as these years were perceived as impacted by below-average rainfall and higher temperatures compared to seasonal averages. The analyses are divided into two parts and are performed at two different scales. The first part is conducted at regional level, encompassing all agricultural areas within the Piedmont region. In this first part, the focus was on assessing crop water stress by evaluating ET during the summer months, which is the period when most seasonal crops are typically cultivated. The results reveal ET values lower than the expected averages, which is the reason why a subsequent analysis at a local scale was conducted. To perform this latter, uniformly cultivated maize areas were identified in the provinces of Turin and Alessandria. In these areas a comparison was conducted between the data collected and processed by MODIS and those calculated using the mathematical model. The estimation of ET through the mathematical model was performed using the maximum and minimum temperature data as well as precipitation data from ARPA. The results highlight a significant discrepancy between the MODIS data and the estimates from the mathematical model in some cases. In particular,

an underestimation of the MODIS product was observed, reaching daily actual ET values of 1mm/day during growing period both at district and local scale. By analysing the potential ET (PET) values of the MODIS product, it appears to be in line with the modelled reference ET (ET0). However, the reduction of PET values to actual ET (calculated as the ET/PET ratio) is very high, with results of about 0.20. The underestimation of ET by MODIS data can be attributed to an indirect measurement of the parameters of aerodynamic resistance, canopy resistance, and soil evaporation, which are considered in the Penman–Monteith equation. In the MODIS algorithm, these parameters are indeed the result of intermediate algorithm calculations. This study aims to contribute to the evaluation of the quality and limiting aspects of the M*D16A2 satellite product on croplands, which has significant potential for large-scale ET estimation and being a ready-to-use product.

Contents

List of Figures

List of Tables

Acronyms

ARPA	Agenzia Regionale per la Protezione Ambientale
CLC	Corine Land Cover
CMG	Climate Modeling Grid
DAAC	Distributed Active Archive Center
EDOS	EOS Data and Operations System
EEA	European Environment Agency
EOS	Earth Observing System
ET	Evapotranspiration
ESA	European Space Agency
FAO	Food and Agriculture Organization of the United Nations
FPAR	Fraction of Photosynthetically Active Radiation
GES DISC	Goddard Earth Sciences Data and Information Services Center
GIS	Geographic Information System
HDF	Hierarchical Data Format
IPCC	Intergovernmental Panel on Climate Change
LAADS DAAC	Level-1 and Atmosphere Archive and Distribution System Distributed Active Archive Center
LAI	Leaf Area Index
MCST	MODIS Characterization Support Team
MODAPS	MODIS Adaptive Processing System
MODIS	Moderate Resolution Imaging Spectroradiometer
NASA	National Aeronautics and Space Administration
NetCDF	Network Common Data Form
NOAA	National Oceanic and Atmospheric Administration
PET	Potential evapotranspiration
QC	Quality Control
RAW	Readily Available Water
SNAP	Sentinel Application Platform
TAW	Total Available Water
TDRSS	Tracking and Data Relay Satellite System

Chapter 1

Introduction

Climate changes represents one of the main environmental problems of the 21st century. According to the sixth Assessment report of IPCC of 2022, a global warming of 1°C has been observed compared to pre-industrial levels and this can be attributed to anthropogenic activities. An average temperature increase of 1.5°C is projected to be exceeded during the 21st century under scenarios involving intermediate, high and very high greenhouse gas emissions [14]. In the long term, a warmer climate alters the balance of the water cycle, affecting evapotranspiration, inter runoff and soil moisture. This translates into a greater climate variability throughout the year and leads to an increase in the frequency of extreme events, like heavy precipitation and floods, hot extremes, drought periods and precipitation deficits [4]. In particular, frequency, intensity, spatial extent, duration, and timing of these extreme events are expected to increase [14].
In addition to their impacts on natural resources, climate changes, along with their inter annual variability, affect economic sectors and lead to human casualties. As regards climate variability and extreme weather conditions, agriculture is the economic sector facing the greatest impact [4]. This is due to the water demand associated with the crop cultivation and the increasing demand for agricultural commodities which is strictly linked to population growth. Indeed, agricultural activities rely on weather conditions for the crop cultivation and the productivity can be strongly altered by climate variability and extreme events. These conditions not only impact rainfed agricultural systems but also irrigated ones, affecting crop yields.
Italy represents an interesting case study for the evaluation of spatial variability of agroclimatic phenomena. It comprises the 20% of the added value of the entire European agricultural system [7] and is significantly affected by the impacts of climate change and climate variability. Furthermore, the country exhibits heterogeneous climatic conditions, diverse soil and topographic characteristics and various structural features within the agricultural sector.

The main challenge that this sector is facing regards the implementation of new approaches to water resource management, ensuring the protection and integrity of the water resources. Increasing water use efficiency has played a leading role in the formulation of strategies aimed to reduce the water allocated for cultivated crops [15]. In this context, the decision to analyse the Piedmont region arises because is an industrialised and agriculturally productive region in Italy. Additionally, in recent years this area was affected by drought events, to which it is not usually subjected. Special attention has been given to the years 2021 and 2022, both affected by positive temperature anomalies and precipitation deficits.
In particular, the year 2021 ranked as the 15th warmest in the past 64 years, with an average temperature of approximately 9.9°C and an average temperature anomaly of around +0.8°C compared to the climatology of the 1971-2000 period. However, for the first time since 2014, there was a spring season with below-average temperatures, breaking a sequence of 26 seasons that had been warmer than the climatology (from autumn 2014 to winter 2021). Total annual precipitation amounted to 858.4 mm, with a deficit of 192.1 mm (equivalent to 18%) compared to the 1971-2000 thirty-year average. Despite this deficit, the region experienced a flood event in the province of Alessandria in October 2021 [21].
On the other hand, the year 2022 was characterised by record-high temperatures and several months of insufficient rainfall. It was classified as the warmest and the second driest in the entire historical series dating back to 1958. It was characterized by a hot and dry climate, unusual for the Piedmont region, with an annual average temperature of 11.4°C and a positive temperature anomaly of 2.3°C compared to the 1971-2000 period. The cumulative precipitation for the year amounted to 611.9 mm, resulting in a precipitation deficit of 438.6 mm (equivalent to 42%) compared to the climatic average of the 1971-2000 thirty-year period [21]. According to reports from ARPA Piemonte, the high temperatures and drought observed in 2022 were unprecedented in the historical context, characterizing this year as affected by a rare and extreme event of intense and diffuse drought. The period assumed significant symbolic value concerning the issue of climate change, capturing the attention of both society and the international media.
To this end, the need to estimate soil evapotranspiration (ET) arises because is a critical parameter for the assessment of crop water stress. Sudden changes in ET values can indicate stress conditions, which might lead to irreversible damages of crops. Thus, the evaluation of ET provides a useful tool for water resource management, agricultural productivity, hydrological modelling and weather forecasting. The precise value of ET is a basic prerequisite for the optimisation of irrigation practices, predict drought conditions and enhance water use efficiency. In the following paragraph, a comprehensive explanation of evapotranspiration, the underlying mechanisms of the process and potential methods for its measurement will be presented.

1.1 Evapotranspiration

Evapotranspiration is the combination of two separate processes whereby water is lost on the one hand from the soil surface by evaporation and on the other hand from the crop by transpiration [1].
Evaporation is the process through which liquid water is converted into water vapour (vaporization) and removed from the evaporating surface. Water can evaporate from different type of surfaces, such as lakes, rivers, pavements, soils and wet vegetation. This process required energy in order to change the state of water molecules and it is supplied by direct solar radiation and, to a lesser extent, by the ambient air temperature. The driving force of evaporation is the difference in pressure between the water vapour at the evaporating surface and that of the surrounding atmosphere. When water evaporates, it releases moisture into the surrounding air, causing the air to become more humid. As the air becomes more saturated with moisture, the rate of evaporation can slow down, and it may eventually stop if the air becomes fully saturated. The replacement of the saturated air with drier air depends greatly on wind speed. Indeed, Wind helps to carry away the moist air and bring in drier air, facilitating the continued evaporation of water. Therefore, solar radiation, air temperature, air humidity and wind speed are climatological parameters to consider when assessing the evaporation process. All of these factors interact to determine the rate and efficiency of the process, making them important considerations in climatological and environmental assessments.
If the evaporating surface is the soil surface, there are other factors that affect the evapotranspiration process like the degree of shading of the crop canopy and the amount of water available at the surface. This latter is influenced by the frequency of rains, irrigation and the transport of water upwards in the soil surface from a shallow water table. Where the soil is able to supply water fast enough to satisfy the evaporation demand, the evaporation from the soil is determined only by the meteorological conditions. However, where the interval between rains and irrigation becomes large and the ability of the soil to conduct moisture to pear the surface is small, the water content in the topsoil drops and the soil surface dries out. Under these circumstances the limited availability of water exerts a controlling influence on soil evaporation. In the absence of any supply of water to the soil surface, evaporation decreases rapidly and may cease almost completely within a few days [1].
The transpiration process is the conversion of liquid water contained in plant tissues into water vapour and its release into the atmosphere. In crops, the loss of water mainly occurs through stomata, that are small openings on the plant leaf through which gases and water vapour pass (Figure 1.1).

Water, along with certain nutrients, is absorbed by the roots and transported throughout the plant. Vaporization occurs within the leaves, specifically in the

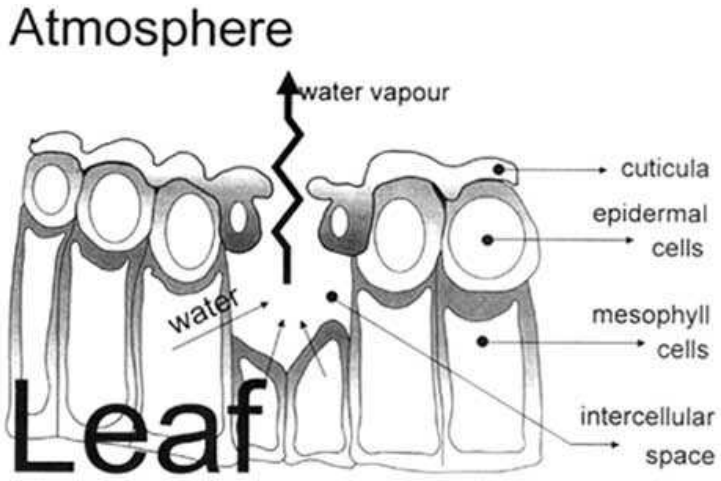

Figure 1.1: Schematic representation of a stoma [1]

intercellular spaces, and the exchange of vapor with the atmosphere is regulated by the stomatal aperture. Almost all of the water absorbed is lost through transpiration, with only a small fraction being utilized within the plant. Transpiration, similar to direct evaporation, is dependent on several factors, including energy supply, vapor pressure gradient and wind. Therefore, parameters like radiation, air temperature, air humidity and wind should be taken into account when assessing transpiration. The transpiration rate is also influenced by soil water content, the ability of the soil to conduct water to the roots, as well as factors like waterlogging and soil water salinity. In addition, the transpiration rate is affected by crop characteristics, environmental conditions and cultivation practices. Therefore, when evaluating transpiration it's fundamental to consider not only the crop type but also its development stage, the surrounding environment and the management practices in place.
In the soil-plant system, evaporation and transpiration occur simultaneously and there is no easy way of distinguishing between the two processes. Besides water availability in the topsoil, the evaporation from a cultivated soil is primarily determined by the fraction of solar radiation reaching the soil surface. This fraction decreases throughout the growing season as the crop develops and the crop canopy progressively shades a larger area of the ground. During the early stages when the crop is small, soil evaporation is the predominant water loss mechanism. However, once the crop reaches full development and completely covers the soil surface, transpiration becomes the main process. In Figure 1.2, the partitioning of evapotranspiration into evaporation and transpiration is displayed in relation to leaf area per unit of soil surface underneath it (*Leaf Area Index*, LAI). At sowing, nearly 100% of ET originates from evaporation, while with full crop canopy

coverage, more than 90% of ET comes from transpiration [1].

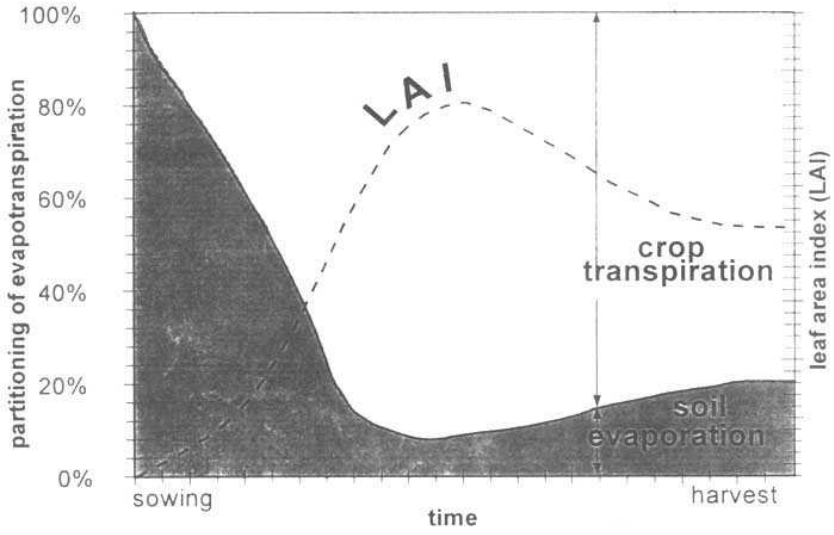

Figure 1.2: The partitioning of evapotranspiration into evaporation and transpiration over the growing period for an annual field crop [1]

The evapotranspiration rate is normally expressed in millimetres (mm) per unit time. The rate expresses the amount of water lost from a cropped surface in units of water depth. The time unit can be an hour, day, decade, month or even an entire growing period or year.
Just as climatic parameters, crop characteristics, and management and environmental factors influence evaporation and transpiration, they also have an impact on evapotranspiration. The main weather parameters affecting ET are radiation, air temperature, humidity and wind speed. Several procedures have been developed to assess the evaporation rate from these parameters. The evaporation power of the atmosphere is expressed by the reference crop evapotranspiration (ET_0), that represents the evapotranspiration from a standardized vegetated surface. The reference crop evapotranspiration, or simply reference evapotranspiration, is the evapotranspiration rate from a reference surface, not short of water. The reference surface is a hypothetical grass reference crop with specific characteristics. The concept of reference evapotranspiration was introduced to assess the atmospheric evaporative demand independently of the crop type, crop development and management practices. Since water is readily available at the reference evapotranspiring surface, soil factors do not significantly affect ET. Associating ET with a specific surface serves as a reference point to which ET from other surfaces can be compared. This obviates the necessity of defining distinct ET levels for each crop and growth stage. Therefore, ET_0 values measured or calculated at different

locations or in different seasons are comparable as they refer to the ET from the same reference surface. ET_0 depends only on climatic parameters and does not consider the crop characteristics and soil factors. For this reason, it can be computed from weather data. The FAO Penman-Monteith method is recommended as the preferred method for calculating reference ET_0. However, this method requires numerous climatic parameters that are not always readily available. For this reason, other reliable methods, such as the Hargreaves-Samani method, can be employed for the assessment of ET_0 when weather data are missing [1].
In the estimation of ET, it is also essential to take into account crop specific factors. Indeed, factors such as the crop type, variety and development stage can significantly affect ET. Differences in resistance to transpiration, crop height, crop roughness, reflection, ground cover and crop rooting characteristics result in different ET levels among different crop types, even when exposed to identical environmental conditions. Crop evapotranspiration under standard conditions, denoted as ET_c, is related to the evaporative demand from crops cultivated in large fields under optimum soil water, excellent management and environmental conditions and achieve maximum potential production under the given climatic conditions.
The amount of water required to compensate the ET loss from the cropped field is defined as crop water requirement. Although the values for crop evapotranspiration and crop water requirement are identical, they refer to different quantities. Crop water requirement refers to the amount of water that needs to be supplied, while crop evapotranspiration refers to the amount of water that is lost through evapotranspiration. The irrigation water requirement basically represents the difference between the crop water requirement and effective precipitation. The irrigation water requirement also includes additional water for leaching of salts and to compensate for non-uniformity of water application. Using the Penman-Monteith approach, crop evapotranspiration can be evaluated from climatic data and by integrating directly the crop resistance, albedo and air resistance factors. This method make use of ET0 to determine the crop evapotranspiration rate, using the formula:

$$ET_c = K_c \, ET_0 \tag{1.1}$$

where K_c is the crop coefficient and it is experimentally determined. K_c incorporates the characteristics that distinguish the reference grass crop from the field crop, and its value depends on the growth stage. In general, crop growth stages can be divided into four main growth stages: initial, crop development, mid-season and late season. The length of each of these stages depends on the climate, latitude, elevation, planting date, crop type, and cultural practices. A schematic representation of the variation of crop coefficient during the growth period is provided in Figure 1.3.
Regarding the management and environmental conditions, there are some factors

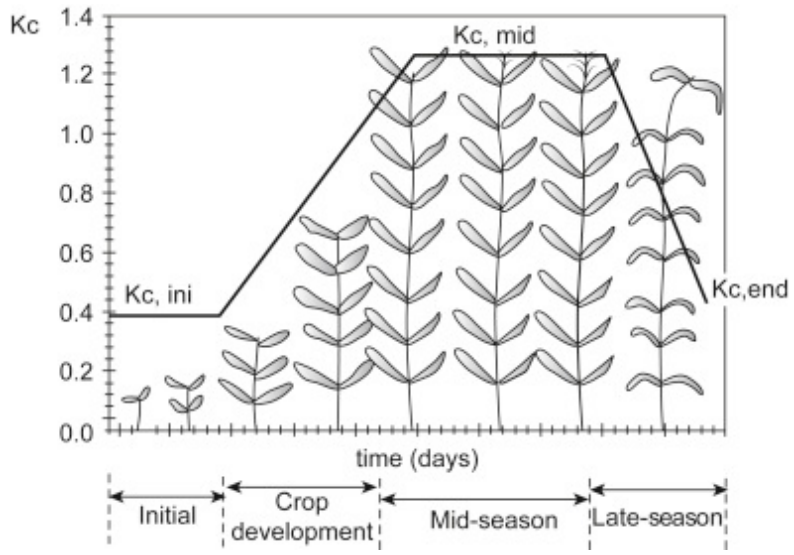

Figure 1.3: Schematic representation of increase and decrease in crop coefficient based on different plant development stages

that affects the ET rate. Soil salinity, poor land fertility, limited application of fertilizers, the presence of hard or impenetrable soil horizons, the absence of control of diseases and pests and poor soil management can constrain crop growth and consequently reduce evapotranspiration. Other factors to consider when assessing ET include ground cover, plant density, and soil water content. The influence of soil water content on ET is primarily determined by the extent of water deficit and the soil type. Conversely, excessive water can lead to waterlogging, potentially harming the roots and constraining root water uptake by inhibiting respiration.
When assessing the ET rate, it is important to consider a range of management practices that impact the climatic and crop factors affecting the ET process. Cultivation practices and the choice of irrigation method can modify the microclimate, influence crop characteristics and affect soil and crop surface moisture levels. For instance, the presence of a windbreak can reduce wind velocities and directly decrease the ET rate in the field just beyond the barrier. This effect can be especially significant in windy, warm and dry conditions, although it's worth noting that evapotranspiration from the trees in the windbreak may offset some of the reduction in the field. In young orchards where trees are spaced widely apart, soil evaporation can be minimized by employing a well-designed drip irrigation system. These systems apply water directly to the soil near the trees, leaving a substantial portion of the soil surface dry and limiting evaporation losses. The use of mulches, particularly when the crop is in its early stages, is another effective way to significantly reduce soil evaporation. Additionally, anti-transpirants, such

as those that close stomata, form films, or have reflective properties, can reduce water losses from the crop and consequently lower the transpiration rate.
Where field conditions differ from the standard conditions, correction factors are required to adjust ET_c. The adjustment reflects the effect on crop evapotranspiration of the environmental and management conditions in the field and result in the actual ET (ET_a). This latter is calculated by using a water stress coefficient K_s on the crop ET and incorporates various stresses and environmental constraints (Equation 1.2).

$$ET_a = K_s\, ET_c \tag{1.2}$$

A schematic representation of the calculation of the reference, crop and actual ET is displayed is Figure 1.4, highlighting the factors that influence them.
For the sake of simplicity in the text, the term *ET* will be used to refer to actual evapotranspiration.

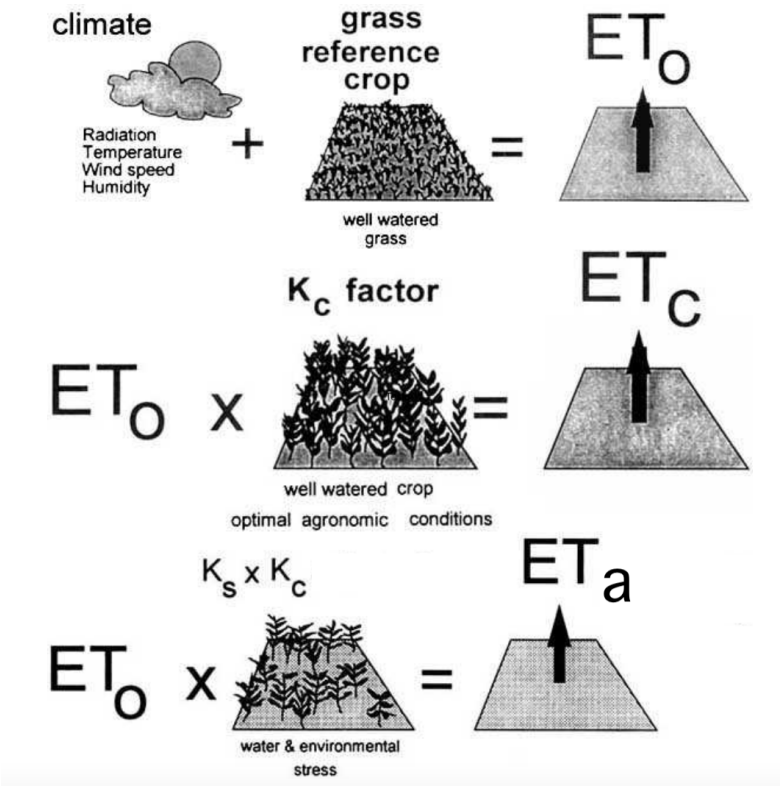

Figure 1.4: Reference (ET_0), crop evapotranspiration under standard (ET_c) and non-standard conditions (ET_a) [1]

Due to its complexity, evapotranspiration is not easy to measure. Indeed, specific instrumentation and accurate measurements of various physical parameters or

the soil water balance in lysimeters are required to determine evapotranspiration. The methods are often expensive, due to the required accuracy of the measurements and the necessity of being carried out by qualified personnel. Although the methods are inappropriate for routine measurements, they remain important for the evaluation of ET estimates obtained by more indirect methods. Direct methods that can be used to measure ET are energy balance and microclimatological methods, soil water balance and lysimeters.
The first method is based on the energy exchanges at the vegetation surface, estimating the evapotranspiration rate by applying the principle of energy conservation. According to this principle, the incoming energy at the surface must equal the outgoing energy for the same time period.
Another method of estimating evapotranspiration is the mass transfer method. In this case the vertical movement of small parcels of air (called *eddies*) above a large homogeneous surface are considered. The eddies transport material (water vapour) and energy (heat, momentum) from and towards the evaporating surface. By assuming steady state conditions and that the eddy transfer coefficients for water vapour are proportional to those for heat and momentum, the evapotranspiration rate can be computed from the vertical gradients of air temperature and water vapour via the Bowen ratio. Other direct measurement methods use gradients of wind speed and water vapour. These methods and other methods such as eddy covariance, require accurate measurement of vapour pressure, and air temperature or wind speed at different levels above the surface. Therefore, their application is restricted to primarily research situations [1].

Evapotranspiration can also be determined by means of the soil water balance. The method consists of assessing the incoming and outgoing water flux into the crop root zone over some time period (Figure 1.5). Irrigation (I) and rainfall (P) represent inputs of water to the root zone. Part of I and P might be lost by surface runoff (RO) and by deep percolation (DP) that will eventually recharge the water table. A vertical water flux might occur through capillary rise (CR) from a shallow water table towards the root zone or even transferred horizontally by subsurface flow in (SF_{in}) or out of (SF_{out}) the root zone. However, SF_{in} and SF_{out} are often negligible compared to others fluxes, with the exception of large slopes. Soil evaporation and crop transpiration deplete water from the root zone. If all fluxes other than evapotranspiration can be assessed, ET can be derived from the change in soil water content (ΔSW) over the time period:

$$ET = I + P - RO - DP + CR \pm \Delta SF \pm \Delta SW \tag{1.3}$$

Some fluxes such as subsurface flow, deep percolation and capillary rise from a water table are difficult to assess and in short time periods are not considered. The soil water balance method is usually adopted for ET estimations over long time periods, of the order of week-long or ten-day periods.

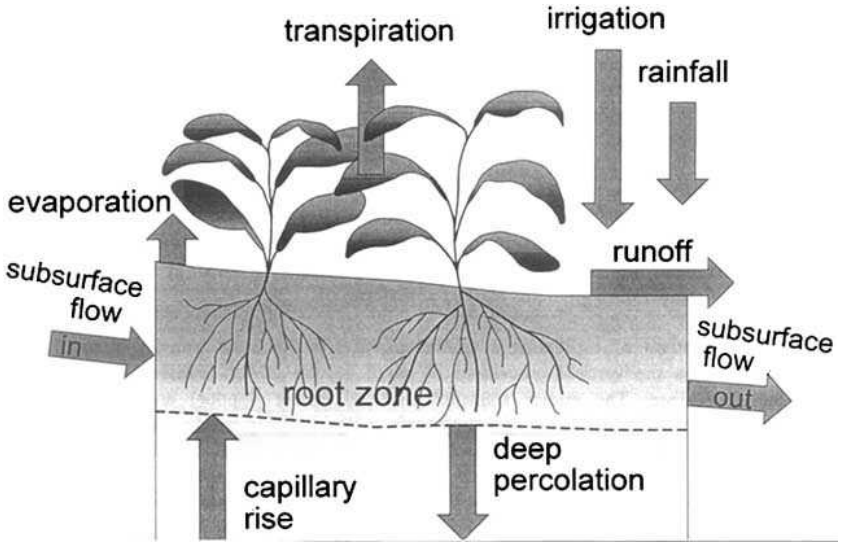

Figure 1.5: Soil water balance of the root zone [1]

Concerning lysimeters, they are devices used for the evaluation of different terms of the soil water balance equation with good accuracy. Their operation is based on isolating the root zone from the environment and controlling processes that are difficult to measure. In lysimeters a crop grows in isolated tanks filled with either disturbed or undisturbed soil. In precision weighing lysimeters, where the water loss is directly measured by changes in mass, ET can be determined with an accuracy of a few hundredths of a millimeter and small time periods (in the order of an hour). In non-weighing lysimeters the evapotranspiration for a given time period is evaluated by subtracting drainage water, collected at the bottom of the lysimeters, from the total water input. A crucial requirement for lysimeters is the uniformity of vegetation both inside and outside the instrument, with same height and LAI. It is proved that if this requirement is not strictly adopted, the instrument detects unrepresentative ET_c and K_c data with significant errors. Lysimeters are challenging and expensive to construct and their operation and maintenance require special care. As a result, their use is limited to specific research purposes. Since it is difficult to evaluate ET from direct measurements, it is commonly computed from weather data. A large number of empirical or semi-empirical equations have been developed for assessing crop or reference crop evapotranspiration from meteorological data. Some of the methods are only valid under specific climatic and agronomic conditions and cannot be applied under conditions different from those under which they were originally developed [1]. However, the scientific community recommends the FAO Penman-Monteith method which was described before.
Another method for estimating ET is through pan evaporation, which involves an open water surface that takes into account the integrated effects of radiation,

air temperature, air humidity, and wind on evapotranspiration. However, it's important to note that this method is significantly influenced by the characteristics of both the water and cropped surfaces. The pan method has demonstrated its practical value and has been successfully used to estimate reference evapotranspiration by monitoring evaporation loss from a water surface and applying empirical coefficients to relate pan evaporation to ET_0.

1.2 Crop water stress

Crop water stress refers to the condition in which a plant experiences an inadequate supply of water to meet its physiological and metabolic needs. This deficiency in water availability can arise from various factors and conditions within the plant's environment. Plants absorb root zone soil water to meet their evapotranspiration needs, and this depletes soil available water. Under limiting soil moisture conditions, chemical and hydraulic signals are transmitted to the plant leaf through xylem pathways, which leads to physiological responses such as stomatal closure and reductions in photosynthesis rate [13]. When a crop is under water stress conditions reduces its evapotranspiration and exhibits other symptoms such as leaf wilting, stunted growth and a reduction of the leaf area. In addition, water stress negatively affects the physiological and nutritional development of crops, leading to a reduction in the biomass, yield and quality of crops.
Thus, evapotranspiration is a critical indicator of crop water stress because it directly reflects the interaction between the crop water demand and the water availability in the root zone. By monitoring ET and its changes over time, it is possible to assess the crop water status. In fact, a sudden decrease in ET can be a signal of water stress conditions and, if evaluated on time, this can allow the implementation of appropriate irrigation practices or the adoption of management measures to mitigate the effects.
According to the FAO method, water stress occurs when the relative soil water content of the root zone approaches an upper threshold value, named *Total Available Water*(TAW). Water content in the root zone can be expressed by root zone depletion, D_r, which is a measure relative to the soil's field capacity. At field capacity the root zone depletion is zero (θ_{FC}), indicating that the plant root zone is fully saturated of water. When soil water is used by evapotranspiration, the depletion gradually increases. The stress is induced at the threshold value, when D_r becomes equal to the *Readily Available Water*(RAW), that is the fraction of TAW that a crop can extract from the root zone without suffering water stress. When the root zone depletion exceeds RAW, evapotranspiration is limited below the potential values and starts to decrease in proportion to the amount of water remaining in the root zone (Figure 1.6) [1]. The effects of water stress on crop

transpiration is described by the water stress coefficient K_s presented in the previous paragraph. When the soil is not under water stress conditions, K_s is equal to 1, while for soil water limiting conditions $K_s<1$. The condition for which K_s is equal to 0 is called *wilting point* and represents the full stress condition.

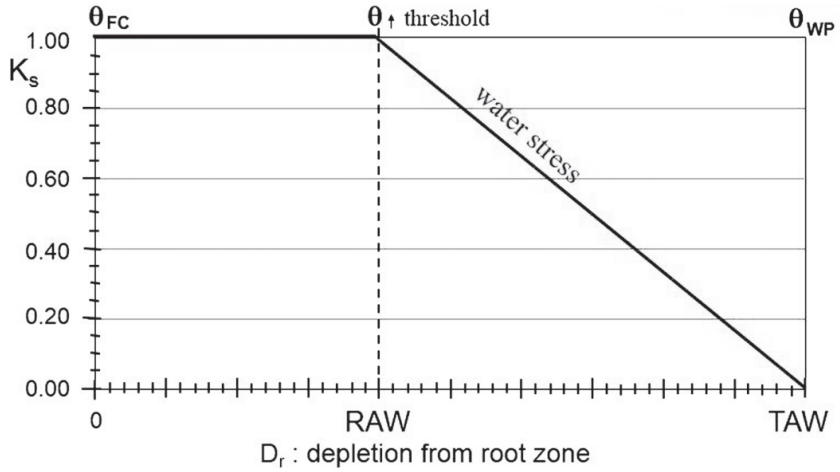

Figure 1.6: Water stress coefficient trend

1.3 Potential satellite-based ET products

Since ET is one of the most difficult components of the water cycle to be determined, the satellite approach proves to be useful in the evaluation of ET at large scales. The satellite earth observation can provide multiple biophysical variables which have a huge potential as input to models or algorithms that are developed to estimate the regional and global ET. In addition, they are able to reflect the impact of land surface heterogeneity and climate variability on ET. However, accurate global ET information or dataset, with spatially and temporally continuous coverage and at moderate resolution, is still scarce [32]. In this section, an overview of the principal satellite-based products containing ET estimations is provided.
The **Global Land Evaporation Amsterdam Model (GLEAM)** is a set of algorithms that separately estimate the different components of evapotranspiration: transpiration, bare-soil evaporation, interception loss, open-water evaporation and sublimation. Additionally, GLEAM provides surface and root-zone soil moisture, potential evaporation and evaporative stress conditions [11]. The rationale of the method is to maximize the recovery of information on evaporation contained in current satellite observations of climatic and environmental variables. It has a spatial resolution of 25 km and a daily temporal resolution. The last version of the data-set covers the entire global surface, spanning the 20-year period from

2003 (January 1st) to 2022 (December 31st). Data-sets are typically updated and extended once a year and are generally released around March. All the GLEAM products are freely available and can be download from the respective website. Another available product is the **Breathing Earth System Simulator (BESS)** evapotranspiration product. BESS is a simplified process-based model that couples atmosphere and canopy radiative transfers, canopy photosynthesis, transpiration and energy balance. The version 2 (v2) of the data-set has a spatial resolution of 1 km and a cumulative 8 days or monthly temporal resolution. BESSv2 includes 1982-2019 data of net radiation, gross primary productivity, terrestrial ecosystem respiration, net ecosystem exchange and evapotranspiration. The data set provides a global coverage and it is freely available [2].
The **LSA SAF (Satellite Application Facility on Land Surface Analysis)**, which is part of the distributed EUMETSAT (European Organization for the Exploitation of Meteorological Satellites) provides another ET products. This latter only covers Europe, Africa and South America and has a spatial resolution of 3 km. Available products include evapotranspiration, reference evapotranspiration and latent and sensible heat fluxes. The temporal coverage of this product ranges between 2004 and near real time. The temporal resolution for evapotranspiration and reference evapotranspiration is at daily scale. Latent and sensible heat fluxes and also evapotranspiration are available with a temporal resolution of 30 minutes [9].
The last ET satellite-based product that is shown is the **MODIS (Moderate Resolution Imaging Spectroradiometer)** evapotranspiration product. This data-set has a daily temporal resolution, but it is provided in cumulative 8-day intervals. It offers global coverage of the Earth with a spatial resolution of 500 meters. Data have been available from 2000 to the present day. There are multiple products for different aspects of the terrestrial water cycle, including evapotranspiration [19]. For the purpose of this study, the MODIS eavpotranspiration product was adopted in the area under analysis. A detailed and comprehensive description of this product will be given Chapter 2, paragraph 2.1.

1.4 Research problem and objectives

The problem to be addressed and investigated in this research is related to the estimation of crop evapotranspiration at a regional scale through the use of a satellite-based product. This approach enables a more cost-effective estimation of ET in terms of instrumentation, time and expertise, while simultaneously proving highly valuable for addressing various spatial and temporal scales. The purpose of this study is to analyse the water stress in the Piedmont region in Italy, which in recent years has been increasingly affected by intense periods of drought, to which

it is not usually subject. The time frame studied includes the two-year period of 2021 and 2022, as they were emblematic from the climatic point of view. In this way, it's also possible to create a continuous time series between two consecutive years without any gaps.
Additionally, the study aims at comparing the performance of the satellite-based MODIS evapotranspiration operational product (M*D16A2) with a mathematical soil water balance model. To achieve this, two types of analyses have been conducted, both at the regional and local scales. The analysis at both scales are of paramount importance, as they complement each other and are both essential for effective and sustainable hydrological management. These analyses provide a comprehensive understanding of hydrological processes in various geographical areas.

1.5 Thesis structure

In addition to this first section, which provides a general introduction to the main themes and the work conducted, this document consists of four additional chapters.
Chapter 2 will present all the materials and data used for this research, with particular emphasis on the MODIS satellite-based evapotranspiration product. In this section, meteorological and agricultural data, as well as all the software used, will also be described.
Chapter 3, on the other hand, will detail the methods employed for data analysis, starting from the calculations underlying the hydrological model to the extraction and handling of satellite data.
Chapter 4 will present the obtained results and their relative discussion, first at a regional scale and then at a local scale.
Finally, in **Chapter 5**, conclusions and future developments of the work undertaken will be reported.

Chapter 2

Material

The analysis of this study include a comparison of ET values between those detected and calculated in a remote way and those estimated by a mathematical model. In the following chapter the data used are described in detail.

2.1 Satellite-based data

MODIS data

Satellite products from NASA's MODIS sensors were used for the analyses. The MODerate Resolution Imaging Spectroradiometer (MODIS) is a satellite-based sensor that provides valuable data for studying different kinds of Earth processes, including evapotranspiration. There are two MODIS sensors in Earth orbit which are mounted on board of two NASA satellites: one on board the *Terra* (formerly EOS AM) satellite launched in 1999 and one on board the *Aqua* (formerly EOS PM) satellite, launched in 2002. MODIS measures several key parameters, such as land surface temperature, vegetation indices and atmospheric properties, that are used to estimate evapotranspiration at regional and global scales. These data will improve our understanding of global dynamics and processes occurring on the land, in the oceans, and in the lower atmosphere. MODIS is playing a vital role in the development of validated, global, interactive Earth system models able to predict global change accurately enough to assist policy makers in making sound decisions concerning the protection of our environment [19].

The MODIS instruments has a viewing swath width of 2,330 km and capture data in 36 spectral bands ranging in wavelength from 0.4 μm to 14.4 μm and at varying spatial resolutions. Observing the entire Earth's surface every 1 to 2 days, these sensors work in tandem to optimize cloud-free surface viewing and provide opportunities to investigate processes that occur on sub-daily time scales [29]. They are designed to provide measurements in large-scale global dynamics

such as changes in Earth's cloud cover, radiation budget and processes occurring in the oceans, on land, and in the lower atmosphere. The MODIS instruments on Terra and Aqua image the same area on Earth approximately three hours apart. Terra's sun-synchronous, near-polar circular orbit is timed to cross the equator from north to south (descending node) at approximately 10:30 A.M. local time. Aqua's sun-synchronous, near-polar circular orbit is timed to cross the equator from south to north (ascending node) at approximately 1:30 P.M. local time [29]. Based on the instruments' orbital cycle, MODIS Land products are distributed at different temporal resolutions. The possible time steps are daily, 4-day, 8-day, 16-day, monthly, quarterly, yearly. MODIS instruments acquire data in three spatial resolutions: 2 bands at 250 m, 5 bands at 500 m and 29 bands at 1 km at nadir. Most of the MODIS Land products use a sinusoidal grid tiling system, that is shown in the Figure 2.1. Tiles are 10 degrees by 10 degrees at the equator. The tile coordinate system starts at (0,0) (horizontal tile number, vertical tile number) in the upper left corner and proceeds right and downward. Higher resolution products with a spatial resolution of 250, 500, and 1,000 meters are organized in non-overlapping tiles based on a sinusoidal grid. There are 460 non-fill tiles covering the globe [20].

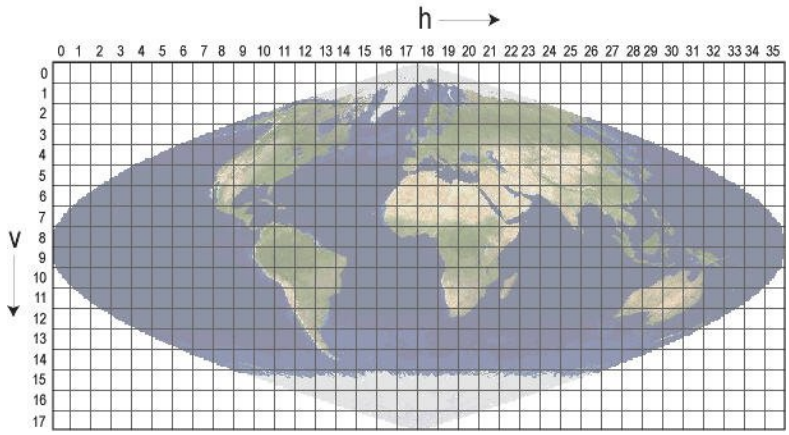

Figure 2.1: MODIS sinusoidal tile grid [20]

Another reference system used by some MODIS products is the climate modeling grid (CMG) which provides a global coverage in a geographic latitude and longitude projection at a resolution of 0.05 degrees (5600 m at the equator). The geographic coordinates of the upper-left corner of the upper-left pixel of a MODIS CMG image are -180.00 degrees longitude, 90.00 degrees latitude. The geographic coordinates of the lower-right corner of the lower right pixel are 180.00 degrees longitude, -90.00 degrees latitude. The CMG is made up of 7200 columns and 3600 rows representing the entire globe for use in climate simulation models [20].

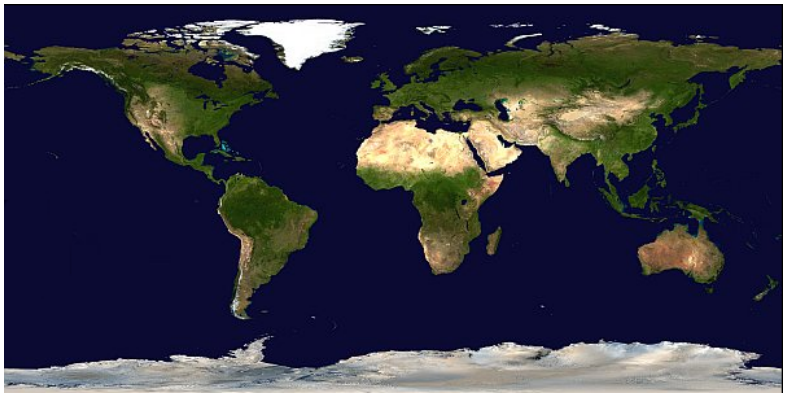

Figure 2.2: Earth surface represented with CMG [20]

MODIS products have various processing levels, ranging from level 2 and above. The possible processing levels are:

- **Level-2**: derived geophysical variables at the same resolution and location as level-1 source data (swath products);
- **Level-2G**: level-2 data mapped on a uniform space-time grid scale (Sinusoidal tile grid);
- **Level-3**: gridded variables in derived spatial and/or temporal resolutions;
- **Level-4**: model output or results from analyses of lower-level data.

All the data collected by the instruments on board the Terra and Aqua platforms are transferred to ground stations in White Sands, New Mexico, via the Tracking and Data Relay Satellite System (TDRSS). Then, data are sent to the EOS Data and Operations System (EDOS) at the Goddard Space Flight Center. Here the level-0 processing is performed and after it the Goddard Earth Sciences Data and Information Services Center (GES DISC) produces the Level 1A, Level 1B, geolocation and cloud mask products. Higher-level MODIS land and atmosphere products are produced by the MODIS Adaptive Processing System (MODAPS) and then are distributed among three DAACs (Distributed Active Archive Center) for distribution. Ocean color products are produced by the Ocean Color Data Processing System (OCDPS) and distributed to the science and applications community [20]. Support and calibration is provided by the MODIS characterization support team (MCST).
MODIS data can be downloaded by the *Level-1 and Atmosphere Archive and Distribution System Distributed Active Archive Center* (LAADS DAAC) web interface [16]. The LAADS DAAC acquires and distributes data on clouds, water vapor and

aerosols in Earth's atmosphere for NASA, NOAA (National Oceanic and Atmospheric Administration) and European Space Administration missions.
The files available for download are in HDF format and there is the possibility to choose the time frame and the world tiles for download. The file naming convention for a tiled product is the following:

M*Dname.AYYYYDDD.hHH.vVV.CCC.YYYYDDDHHMMSS.hdf

where the first part of the file name (M*D16name) identifies the product name and gives information about the satellite of acquisition. The acronym *MYD* refers to product acquired by the AQUA satellite while the acronym *MOD* for those of the TERRA satellite. The A stand for date of acquisition and it's followed by the year and day of year of acquisition (YYYYDDD). The hHH and vVV parts refer to the horizontal (0-35) and vertical (0-17) tile number respectively. Then, it follows the collection version (CCC) and the YYYYDDDHHMMSS section that indicates the processing year (YYYY), Julian day (DDD), hour (HH), minute (MM), and second (SS) of the data processing. A list of all the available MODIS products is provided in Table 2.1.

Calibration	M*D01	Level-1A Radiance Counts
	M*D02	Level-1B Calibrated Geolocated Radiances
	M*D03	Geolocation Data Set
Atmosphere	M*D04	Aerosol Product
	M*D05	Water Vapour
	M*D06	Cloud Product
	M*D07	Atmospheric Profiles
	M*D08	Gridded Atmospheric Product
	M*D35	Cloud Mask
Land	M*D09	Surface Reflectance
	M*D11	Land Surface Temperature and Emissivity
	M*D11	Land Cover/Change
	M*D13	Gridded Vegetation Indices
	M*D14	Thermal Anomalies, Fires and Biomass Burning
	M*D15	Leaf Area Index and FPAR
	M*D16	Evapotranspiration
	M*D17	Net Photosynthesis and Primary Productivity
	M*D43	Surface Reflectance
	M*D44	Vegetation Cover Conversion

Cryosphere	M*D10	Snow Cover
	M*D29	Sea Ice Cover
Ocean	M*D18	Normalized Water-leaving Radiance
	M*D19	Pigment Concentration
	M*D20	Chlorophyll Fluorescence
	M*D21	Chlorophyll Pigment Concentration
	M*D22	Photosynthetically Available Radiation (PAR)
	M*D23	Suspended Solids Concentration
	M*D24	Organic Matter Concentration
	M*D25	Coccolith Concentration
	M*D26	Ocean Water Attenuation Coefficient
	M*D27	Ocean Primary Productivity
	M*D28	Sea Surface Temperature
	M*D31	Phycoerythrin Concentration
	M*D36	Total Absorption Coefficient
	M*D37	Ocean Aerosol Properties
	M*D39	Clear Water Epsilon

Table 2.1: Standard MODIS products

2.1.1 MODIS ET Product (M*D16) collection 6.1

For the purpose of this study the MODIS product 16A2 of the collection 6.1 was used. The collection 6.1 is the latest version released in 2021, that differs from the previous one (collection 6) in the calibration processing. Some changes and enhancements were performed to the calibration approach used in generation of the Terra and Aqua MODIS L1B products and changes to the polarization correction used in this collection reprocessing. The satellite products 16A2 belong to the MODIS Land Surface Evapotranspiration (ET) algorithm suite. Both MOD16A2 and MYD16A2 products provide estimations at a 500 m spatial resolution and an 8-day temporal resolution. With a global coverage of 109.03 Million km^2 global vegetated land areas, they are valuable tools for assessing temporal and spatial water and energy balance. The data-set covers the time period from 2000 to present and, since it is a level 4 EOS data product, the grid data sets are saved in sinusoidal map projection. In addition to ET, other parameters are evaluated in these data-sets that also provide key information for soil water status and hence water resource management: potential ET (PET), latent heat flux (LE), and potential LE (PLE). ET and PET are the summation of total daily ET or PET through the year (0.1 $kg/m^2/year$) whereas LE and PLE are the corresponding average total latent energy over a unit area for a unit day (10000 $J/m^2/day$) through the year. The real

value of each variable in the corresponding units can be calculated by multiplying the valid data for the corresponding scale factor. More details about the variables are summarized in Table 2.2.

Name	Description	Units	Valid Range	Scale factor
ET	Total evapotranspiration	kg/m²/8day	-32767 to 32700	0.1
LE	Average latent heat flux	J/m²/day	-32767 to 32700	10000
PET	Total potential evapotranspiration	kg/m²/8day	-32767 to 32700	0.1
PLE	Average potential latent heat flux	J/m²/day	-32767 to 32700	10000

Table 2.2: Detailed information on data sets in M*D16A2

In this study only the ET and PET products were used.

The algorithm

Total ET includes evaporation from wet and moist soil, from rain water intercepted by the canopy before it reaches the ground and the transpiration through stomata on plant leaves and stems. In the computation of ET there are two major issues: estimation of the canopy conductance to derive transpiration from plant surfaces estimation of evaporation from the soil surface.

The MOD16 algorithm is based on the logic of the Penman-Monteith equation and it uses daily meteorological reanalysis data and 8-day remotely sensed vegetation property dynamics from MODIS as inputs. In particular, meteorological input data are air pressure, air temperature, humidity and solar radiation while remotely sensed ones are land cover, leaf area index (LAI) and albedo. The algorithm runs at daily basis and temporally, daily ET results from the sum of ET from daytime and night. Vertically, ET is the sum of water vapour fluxes from soil evaporation, wet canopy evaporation and plant transpiration at dry canopy surface. The MOD16A2 and MYD16A2 products make use of a two-source energy balance model that takes into account various factors influencing evapotranspiration, such as incoming solar radiation, air temperature, surface temperature, and vegetation cover. These data inputs are integrated to estimate the amount of water vapour transpired by the land surface. The result is a comprehensive representation of evapotranspiration dynamics over large areas, enabling scientists to analyse trends and patterns. Figure 2.3shows the logic behind the MOD16 ET Algorithm for the evaluation of evapotranspiration.

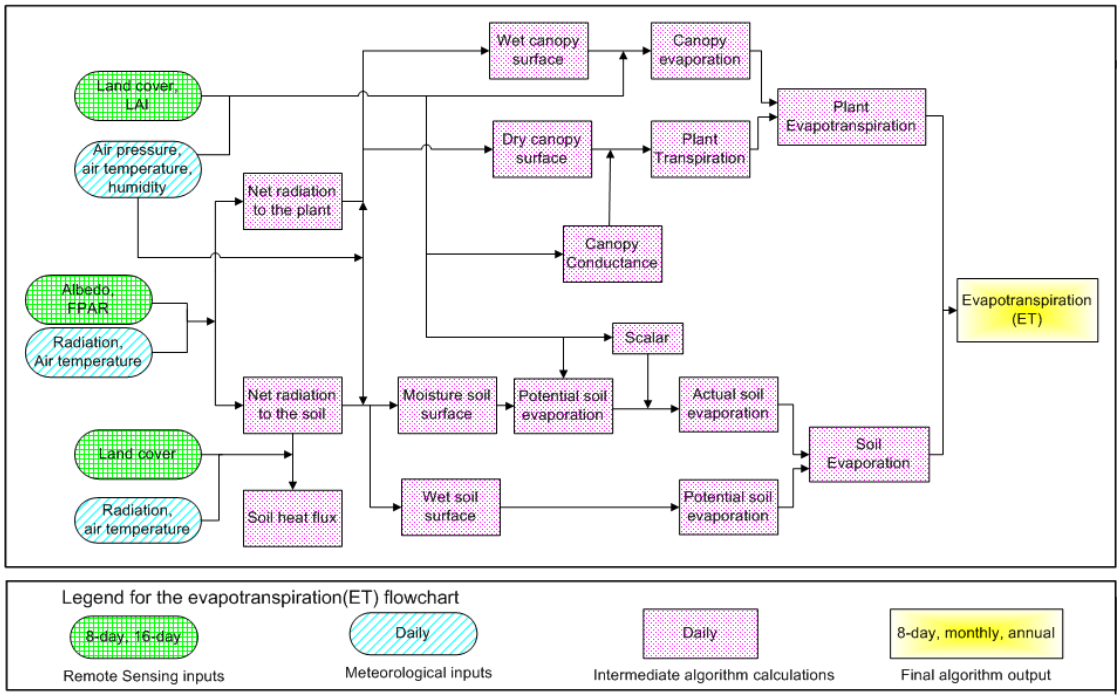

Figure 2.3: Flowchart of the MOD16 ET algorithm.

Gap filled product

The M*D16A2 has an improved product, named *Gap filled*, which is equal in terms of acquired parameters and spatial and temporal resolutions but which has cleaned the poor-quality inputs from 8-day Leaf Area Index and Fraction of Photosynthetically Active Radiation (LAI/FPAR) based on the Quality Control (QC) label for every pixel. In particular, if any LAI/FPAR pixel did not meet the quality screening criteria, its value is determined through linear interpolation [20].
The improved product is distinguished from the non-gap-filled one by the data product's name, to which "GF" is added to the names of the data files, such as M*D16A2GF. It is a year-end 8 day composite dataset, meaning that it's released at the end of each year, when the entire yearly 8-day M*D15A2H is available. This is the limitation of the gap-filled product since it doesn't allow the analysis of current-year data but only data from previous years.
As for the M*D16A2 product, the parameters estimated by the gap-filled one are evapotranspiration (ET), latent heat (LE), potential ET (PET) and potential LE (PLE). The pixel values for the ET and PET are the sum of all eight days within the composite period while the pixel values for LE and PLE are the average of all eight days within the composite period. Depending on whether the year is leap or not, the last acquisition period of each year is a 5- or 6-day composite period.

Also in this product the coordinate system is sinusoidal and the valid range and scale factor are the same of M*D16A2.

2.2 Meteorological data

2.2.1 ARPA

In order to compare the evapotranspiration value retrieved by the satellite product with a theoretical estimation, it was used a mathematical model which will be described in Chapter 3. The input meteorological parameters of the model are: latitude, daily precipitation, minimum and maximum temperature. All these data were taken by Arpa Piemonte, that is *Agenzia Regionale per la Protezione Ambientale*. It is a public body in the Piedmont region of Italy with administrative, technical-legal, patrimonial and accounting autonomy. Its aim is to ensure the implementation of the programmatic guidelines of the Piedmont Region in the field of environmental forecasting, prevention and protection [21]. ARPA Piemonte's primary objective is to monitor and assess environmental quality, analyze data, and provide reliable information to policymakers, researchers, and the public. The agency covers a wide range of environmental domains, including air quality, water resources, soil, noise pollution, and climate change. By collecting and disseminating accurate data, ARPA Piemonte contributes to evidence-based decision-making aimed at preserving the region's natural resources. Environmental monitoring is the main function of ARPA Piemonte, which is done by means of a network of monitoring stations located over the region. In this way ARPA is able to gather real-time data on environmental parameters. This survey is crucial for assessing compliance with environmental regulations, identifying pollution sources and evaluating the effectiveness of pollution control measures. All the data acquired by the ARPA stations are accessible and downloadable by everyone through the website. Two types of data from ARPA were used in this study, ground station data and NWIOI gridded data-set, which are described in the following paragraphs.

2.2.2 Data from ground stations

The first option is to use daily data directly measured by ground stations. It is possible to access to these data in two ways: by the historical database (*Banca dati storica*) or by making a request in the designated section of the website [22]. In both cases, once the interested district is chosen, a list of all the stations located in different municipalities of the district appears and the one of interest can be selected. It should be noted that not all stations are equipped with the same instruments, therefore it may happen that the selected location does not register the parameters of interest.

2.2.3 NWIOI gridded data

The NWIOI gridded data-set contains daily data of cumulative precipitation, minimum and maximum temperature that are calculated and interpolated on a regular grid which covers the entire region. The interpolated data are the result of those recorded by the stations. The data-set is maintained and updated daily by ARPA Piemonte's Forecasting Systems Department [23]. Data are gathered together in three files, one for each variable and they cover a time frame that goes from 1/12/1957 until yesterday. All the files are daily updated after 6:00 pm.
The data are distributed as Open-Data under the Creative Commons BY 2.5 Italian standard license. The file format is NetCDF (Network Common Data Form), Binary format supported by special libraries and widely used in the scientific field. Other characteristics of the NWIOI gridded data are summarize din the following table:

Longitude extension	6.5-9.5 W
Latitude extension	44.0-46.5 N
Resolution	0.125°
Geographic reference system	WGS84 lat lon (EPSG:4326)

Table 2.3: Characteristics of NWIOI gridded data [23]

Since this type of data is spatially interpolated and, therefore, more regular, it is preferable when analysing a location that is not covered by a meteorological station or does not have one nearby.

2.3 Agricultural data

In order to determine the agricultural area in the Piedmont region, the Corine Land Cover 2018 (CLC2018) data-set was used. The CLC program, which is part of the Copernicus program, is an initiative of the European Environment Agency (EEA) to produce a pan-European land cover and land use data-set. The objective is to provide detailed information on land cover and land use across Europe, with the data updated at regular intervals. It plays a crucial role in environmental monitoring, policy development and research in various domains. The data-set produced by CLC is freely available and can be accessed through the Copernicus Land Monitoring Service website[5]. The spatial resolution and nomenclature of CLC have not changed during its lifetime, thus maintaining the comparability between consecutive inventories. The spatial resolution is 100 m and the minimum mapping unit is 25 ha for mapping status layers, meaning that objects having less than 25 ha area can not be present in the database [5]. The

nomenclature is hierarchical and includes three levels of thematic detail in five main groups:

- Artificial surfaces
- Agricultural areas
- Forests and semi-natural areas
- Wetlands
- Water bodies

In addition to pure land cover classes, the nomenclature includes land use classes, while some classes have a mixed land cover/land use character. At the end there are 44 classes on level-3 [5]. This classification can be very useful in understanding land use changes and assessing the impact of land use on the environment. For this analysis, the extracted categories were *agricultural land* and *forest and semi-natural areas* in order to analyse all the vegetated areas of the region. All the classes belonging to these two groups are set out in more detail below.

Level 1	**Level 2**	**Level 3**
1 Artificial surfaces	11 Urban fabric	111 Continuous urban fabric
		112 Discontinuous urban fabric
	12 Industrial, commercial and transport units	121 Industrial or commercial units
		122 Road and rail networks and associated land
		123 Port areas
		124 Airports
	13 Mine, dump and construction sites	131 Mineral extraction sites
		132 Dumps sites
		133 Construction sites
	14 Artificial, non-agricultural vegetated areas	141 Green urban areas
		142 Sport and leisure facilities
2 Agricultural areas	21 Arable land	211 Non-irrigated arable land
		212 Permanently irrigated land
		213 Rice fields
	22 Permanent crops	221 Vineyards
		222 Fruit trees and berry plantations
		223 Olive groves

Level 1	Level 2	Level 3
	23 Pastures	231 Pastures
	24 Heterogeneous agricultural areas	241 Annual crops associated with permanent crops
		242 Complex cultivation patterns
		243 Land principally occupied by agriculture, with significant areas of natural vegetation
		244 Agro-forestry areas
3 Forest and semi natural areas	31 Forests	311 Broad-leaved forest
		312 Coniferous forest
		313 Mixed forest
	32 Scrub and/or herbaceous vegetation associations	321 Natural grassland
		322 Moors and heatland
		323 Sclerophyllous vegetation
		324 Transitional woodland-shrub
	33 Open spaces with little or no vegetation	331 Beaches, dunes sands
		332 Bare rocks
		333 Sparsely vegetated areas
		334 Burnt areas
		335 Glaciers and perpetual snow
4 Wetlands	41 Inland wetlands	411 Inland marshes
		412 Peat bogs
	42 Maritime wetlands	421 Salt marshes
		422 Salines
		423 Intertidal flats
5 Water bodies	51 Inland waters	511 Water courses
		512 Water bodies
	52 Marine waters	521 Coastal lagoons
		522 Estuaries
		523 Sea and ocean

Table 2.4: Corine Land Cover nomenclature [5]

For the analysis at the local scale, it was decided to observe the response of a single crop. In this instance, maize was selected since the Piedmont region is the third producer and cultivator in Italy [28]. Therefore, a research was conducted to determine which lands were cultivated with maize using *Anagrafe agricola* made available by Regione Piemonte [24]. The latter can be accessed on the *Geoportale Piemonte* [25] by using the *Uso del suolo agricolo su mosaicatura catastale di*

riferimento regionale layer and downloading the data for the year and area of interest. The data is presented on a digital map, which can be accessed online or, in the case of downloading, can be read by software capable of analyzing spatial data and cartography. At this stage, it is possible to filter the data based on the type of crop.

2.4 Software

In this section all the software used for the analysis are described.

2.4.1 SNAP

The Sentinel Application Platform (SNAP) is an open-source software developed and provided by the European Space Agency (ESA) to support the processing, analysis and visualization of data from the Sentinel satellites within the Copernicus program. This software is a comprehensive and powerful tool for professionals in several fields, such as remote sensing, Earth observation and environmental monitoring. SNAP allows to processing and analyse satellite data due to the following technological innovations: extensibility, portability, modular rich client platform, generic earth observation data abstraction, tiled memory management and a graph processing framework [8]. It is able to handle data from multiple satellite missions and supports various data formats. In this study SNAP was used to visualize MODIS data and extract the numerical values of the variables of interest.

2.4.2 MATLAB

MATLAB is a programming and numerical computing platform developed by MathWorks and used for data analysis, algorithm development and creation of models [17]. In this context, it was used for data manipulation, implementation of algorithms and plotting. All the analyses of MODIS data were performed by means of MATLAB, as well as most of the graphical outputs.

2.4.3 QGIS

QGIS is a free and open-source geographic information system (GIS) desktop application that supports viewing, creating, editing, printing, and analysis of geospatial information [26]. It was used for the representation of results along with their associated geographical information.

Chapter 3

Methods

The following chapter describes the methods used for the estimation of actual ET by means of the mathematical model and the processes adopted for the extraction of ET and PET values from the satellite products.

3.1 Estimation of the theoretical ET through a mathematical model

For the evaluation of the theoretical evapotranspiration, both the reference and the actual ones, it was used a MATLAB model created and written by the engineer Matteo Rolle based on the previous studies of Marta Tuninetti. The mathematical model estimates crop growth and irrigation requirements for 26 main crops and for 10 climatic regions. The model computes a soil water balance using daily precipitation and reference evapotranspiration based on a high-resolution ERA5 reanalysis data-set from the European Copernicus Program. The irrigation requirement is defined as the minimum water volume to avoid water stress [27].
The code is divided in three parts: one for the estimation of the reference evapotranspiration (ET_0) and the other two for the evaluation of the actual evapotranspiration (ETa) in rainfed or irrigated conditions. All the models are described in the following paragraphs.

3.1.1 Estimation of ET_0

The evaluation of the reference ET is performed using the Hargreaves-Samani formula (1985) (Eq. 3.1). This method is often used to provide ET_0 predictions for weekly or longer periods for use in regional planning, reservoir operation studies, canal design capacities, regional requirements for irrigation and/or drainage, potentials for rainfed agricultural production and for irrigation scheduling. The

attractiveness of the method is its simplicity, reliability, minimum data requirements, ease of computation, and low impact by aridity conditions. The Eq. 3.1 is also widely used when only air temperature data are available [12].

$$ET_0 = 0.0023\, R_a (T_m + 17.8)\sqrt{\Delta T} \tag{3.1}$$

The input in the model are the maximum and minimum air temperature and the latitude of the cell. Starting from the latter parameter, the model is able to evaluate the extraterrestrial radiation R_a. Then, by means of the Eq. 3.1 the reference ET is calculated. In Eq. 3.1 T_m refers to the average temperature while ΔT to the difference between the maximum and minimum temperature.

3.1.2 Estimation of ET_a

The mathematical model for the evaluation of actual ET is based on the FAO guidelines (FAO n.56, Allen et al. 1998), both for rainfed and irrigated conditions [1]. The equation used is the following:

$$ET_a = ET_0\, k_c\, k_s \tag{3.2}$$

where ET_0 is the reference evapotranspiration, k_c the crop coefficient and k_s the water stress coefficient. The input parameters both for rainfed and irrigated conditions are: crop type, climate region, sowing and harvesting dates, daily precipitation and reference ET and soil characteristics. These latter consists in the initial soil moisture, sowing soil moisture and available water capacity. The first one is the value obtained from the soil water balance of the previous day while the sowing soil moisture is evaluated at the sowing day for temporary crops or set as 0 for perennial crops. In this case, the soil water balance only requires an initial daily soil moisture because no sowing occurs. In the case under study, only rainfed maize fields are analysed with this model and the Piedmont region is classified with a sub-continental temperate climate [18]. The sowing and harvest dates are set based on previous studies and on FAO database [10] [27]. Daily precipitation data are taken from ARPA [21] while the input reference evapotranspiration is calculated with the previous method (see paragraph 3.1.1). The initial and sowing soil moisture and the available water capacity are instead retrieved from the *Soil Water Index* data-set distributed by the *Copernicus Global Land Service* [6]. The output for both models are the final soil moisture and the actual ET. In irrigated conditions, ET_a is the sum of two contributes, the evapotranspirative requirement fulfilled by precipitation water (ET_{prec}) and the daily irrigation required (Irr_{req}) to avoid crop water stress condition. The unit of measurement of all inputs and outputs of the mathematical model are listed in the table below.

Input	**Unit of measurement**
Crop type	-
Climate region	-
Sowing and harvest dates	-
Precipitation	mm/day
ET_0	mm/day
Initial soil moisture	m^3 of water/m^3 of soil
Sowing soil moisture	m^3 of water/m^3 of soil
Available water capacity	m^3 of water/m^3 of soil

Output	**Unit of measurement**
Final soil moisture	m^3 of water/m^3 of soil
ET_a	mm/day
ET_{prec}	mm/day
Irr_{req}	mm/day

Table 3.1: Units of measurements of inputs and outputs of the mathematical soil water balance model

Since the outputs from the mathematical models are provided at a daily scale, they are upscaled to cumulative values over 8-day periods for the purpose of comparison with MODIS satellite data.

3.2 MODIS data analysis

The analysis of MODIS data can be subdivided in two methods: one used for the regional analysis and the other one for local study.

3.2.1 Regional analysis

The analysis is conducted in MATLAB following the subsequent steps. Initially, a raster image identical to the MODIS tile is loaded, in which the pixels contain only values of 0 and 1. Pixels with a value of 1 represent the areas to be analyzed, whereas pixels with a value of 0 indicate those to be excluded. In this way, a mask has been created that can be applied to all other files. The raster image is read using the *readgeoraster* function, which creates a matrix of data values along with the corresponding spatial reference system. Subsequently, all files of a MODIS

product for an entire year are read through a *for* loop. Each file is read using the *hdfread* function, specifying the band to be subsequently extracted (in this case, the ET_500m and PET_500m bands were used), and multiplied by the corresponding scale factor. Then, the mask created in advance is applied by multiplying the file matrix by the mask matrix. The result is a matrix of the same dimensions as the original containing MODIS values in the pixels of the areas under analysis and zero values in the excluded areas. Once these procedures have been applied to all files for a year using a *for* loop, a set of 46 matrices is generated, containing values for only the areas under study. Then, all the matrices covering one year are saved in a 3D matrix in which the first and second dimensions represent respectively the longitude and latitude while the third dimension represents the time. In this way, it is created an annual data-set that can be managed and on which is possible to perform various operations. Once the desired operations are completed, the final matrix is exported in a NetCDF file using the MATLAB *high-level netCDF* functions. The spatial reference system is specified in the file's attributes. At this point, the file can be imported into QGIS for better visualization and the addition of cartographic elements.
This method has been employed for each year of each analyzed satellite product of this study.

3.2.2 Local analysis

For the local-scale analysis, a different approach was adopted. First, after selecting the area to be analyzed using the *Anagrafe agricola* from *Geoportale Piemonte*, a corresponding vector was created in QGIS software. The area selection is made by identifying cultivated fields that are as uniform as possible and have dimensions of about 500m x 500m, so that they can be represented by a single pixel in the satellite image. After this, the extraction of the MODIS ET and PET values is performed by means of SNAP. Once the HDF files are downloaded from the LAADS DAAC web interface [16] (see paragraph 2.1, pp 5-6), they are opened with the SNAP software. As the values to be analyzed cover specific pixel of the MODIS dataset, the *Graph Builder* and *Batch Processing* tools have been employed in conjunction to extract only the values pertaining to the areas under analysis. The Graph Builder tool offers the possibility to apply the same order of commands to more than one image. In particular, the *Import- Vector* function was used, specifying the directory of the initially created file. The process of the graph builder is displayed in Figure 3.1.

Then, through the Batch Processing tool, the graph builder is applied to all the files intended for analysis. In the case of this study, one year of each satellite product was analyzed at a time. After loading the masks of the fields to be analyzed, a pin is placed at the location of each mask. With the SNAP time series

Figure 3.1: Graph Builder in SNAP

tool, it is possible to extract the values of the selected parameters (in this study, ET and PET) from all the files loaded using the batch processing. The extracted data is then exported and saved in a CSV file. At this point, the latter file can be loaded and read in MATLAB, providing the opportunity to manage data, perform various operations, and visualize it graphically.

Chapter 4

Results and discussion

4.1 Area under study

The area under study includes the Piedmont region, which is located in the North-West of Italy. With an extension of 25 402 km^2, it's the second biggest region in Italy. Piedmont is located beneath the western Alps, which surround it on all the sides with the exception of the eastern side. Almost half of the territory is mountainous (43.3%), followed by extensive areas of hills (30.3%) and plains (26.4%). Thanks to this variety of landscapes, Piedmont exhibits various types of climates, although the regional one is classified as temperate subcontinental [18]. This leads to different contributions to the country's agrarian sector, with a rich mosaic of agricultural opportunities. The extension of agricultural areas in Piedmont is significant, with an extension of 923,428 hectares designated for agricultural production. The plains of the Po Valley is the primary focus of cereal and rice cultivation while the hilly and mountainous areas are conducive to viticulture and fruit orchards. This geographic diversity allows the production of a wide array of agricultural products where the primary cultivated crops are grapes, wheat, maize, rice and hazelnuts.
Regarding maize production, Italy in one of the major producers in Europe. It is used for both human consumption and animal feed, as well as a crucial raw material for various industries. In 2019, Italy had a maize cultivation of approximately 630,000 hectares and a production of 6.4 million tons. 73% of the national production is concentrated in northern Italy, with the Piedmont region ranking as the third-largest producer [28].

The agricultural census of 2020 highlighted that in that year, Piedmont had 15,167 maize businesses and 147,038 hectares of crops cultivated with maize, representing 26% of the total cultivated crops [3].

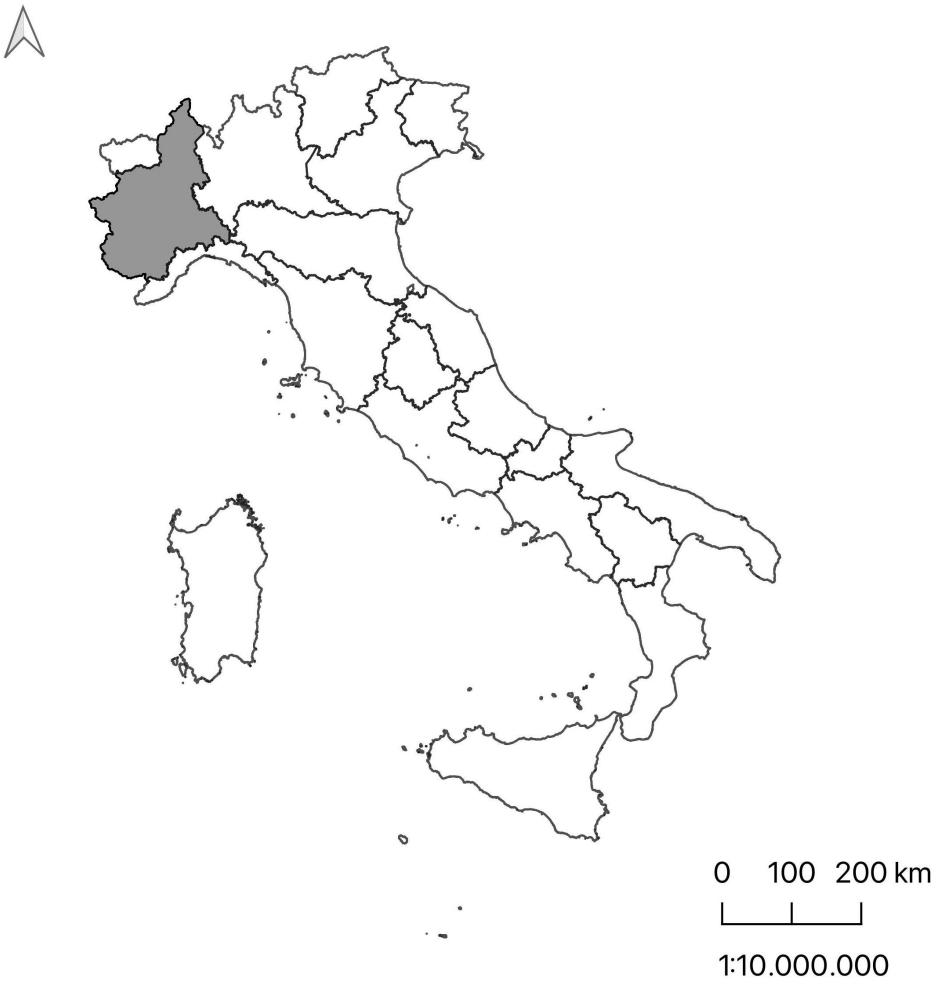

Figure 4.1: Piedmont, Italy

4.2 Maize

Maize, known scientifically as *Zea mays*, is one of the most important cereal crops both for human and animal consumption and is grown for grain and forage. Due to its easy adaptability to different climatic conditions, maize is cultivated worldwide, accounting for a total global production of 594 million tons grain from about 139 million ha [10]. The crop is grown in climates ranging from temperate to tropical, during the period when mean daily temperatures remain above 15°C and frost is absent. It is essential to choose the right variety to match the crop's growing period with the length of the local growing season.
Regarding temperature, for germination maize requires a minimum mean daily

temperature of about 10°C, with an optimum range between 18 to 20°C. The crop is highly sensitive to frost, especially during the seedling stage, but it tolerates hot and dry atmospheric conditions as long as an adequate water supply is available to the plant and temperatures remain below 45°C. Higher temperatures generally result in a shorter growth phase for maize. The crop thrives in mean daily temperatures ranging from 15 to 20°C. In regions where the mean daily temperature is between 10 and 15°C, maize is mainly grown as a forage due to challenges related to seed development and grain maturity under cooler conditions.
The maize plant thrives in a variety of soil types but performs less effectively in extremely heavy, compacted clay soils and excessively sandy soils. Ideally, the soil should be well-aerated and have good drainage capacity, as maize is susceptible to waterlogging.
In the following table are summarized the key crop coefficients used in water management.

Crop characteristic	**Initial**	**Crop development**	**Mid-season**	**Late**	**Total**
Stage length, days	25	40	40	35	140
Depletion coefficient, p	0.5	0.5	0.5	0.8	-
Root Depth, m	0.30	»	»	1.00	-
Crop Coefficient, Kc	0.30	»	1.2	0.5	-
Yield Response Factor, Ky	0.40	1.40	1.30	0.5	1.25

Table 4.1: Key parameters of maize based on development stages [10]

Maize uses water efficiently in terms of total dry matter production, and among cereals, it has the potential to yield the highest grain production. To achieve maximum production, a medium-maturity grain crop typically requires between 500 and 800 mm of water, depending on the climate. On average, maize evapotranspiration rates during the central stages of development correspond to 5-6 mm/day [10].

4.3 Regional analysis of agricultural areas

The regional analysis was conducted for the two-year period 2021-2022, as these years were perceived as drought years, and consequently, years in which the effects on evapotranspiration should be more pronounced. The decision to study all the agricultural areas of the region comes from the will to assess whether the MODIS satellite product could serve as a reliable tool for quantifying ET on a large scale. The extent of the cultivated areas was estimated using the Corine Land Cover 2018 data-set and is depicted in Figure 4.2.

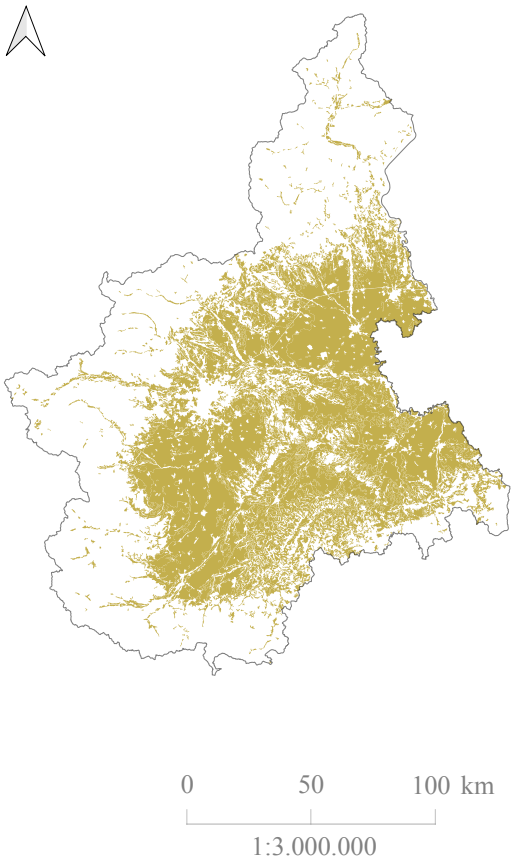

Figure 4.2: Agricultural areas in Piedmont [5]

The satellite data available for the analysis consist of four datasets for each year: the product derived from the TERRA satellite, the one from the AQUA satellite, and their two respective gap-filled products. In this regard, a data availability analysis was conducted to determine which product was most suitable for the purpose. The data availability analysis was conducted exclusively on the non-gap-filled products because the gap-filled ones have not cleaned the poor-quality inputs from the LAI/FPAR product (M*D15A2). In fact, the gap-filled products contain data for the entire year without interruptions. Conversely, the non-gap-filled products also include detections from non-vegetated pixels. These detections can be readily identified, as the MODIS algorithm assigns unreasonably high ET values to non-vegetated areas within the 8-day time frame. In the following table, six fill values are listed for non-vegetated pixels, for which ET is not calculated (Table 4.2).

Fill value	Land cover assigned as
32761	Unclassified
32762	Urban/Built-up
32763	Permanent wetlands
32764	Perennial snow/ice
32765	Barren, sparse vegetation or used for data gaps from cloud cover or snow for vegetated pixel
32766	Perennial salt/water bodies

Table 4.2: Detailed information on fill values in M*D16A2 data-set [30]

As the availability data analysis encompasses only already classified vegetated areas, the only anomalous pixel values that may be encountered correspond to cloud or snow cover (fill value=32756). The fact that the satellite is not able to collect data in the presence of cloud or snow cover represents a significant limitation.
To assess data availability on an annual basis, all anomalous ET values for each individual pixel within the cultivated areas were excluded. Subsequently, the percentage of available data over a one-year time frame was calculated, ranging from 0 (no data available) to 100 (all data available). The results were visualized on a map, with a color scale associated with the percentage values (Figure 4.3-4.4). As can be observed, in all four maps, the northeast area of the region is characterized by a lower data presence. This could be attributed to the high concentration of rice paddies in that area, where differing soil reflectance may influence satellite detection. Indeed, in these areas, there is a peak of lower data availability, with approximately 40% of annual data availability.
Furthermore, variations are noticeable both between the two years and between the two satellite products. Concerning the two satellite products, data from the TERRA satellite are higher compared to those from the AQUA satellite for both years. This may be attributed to the differing orbital pass times of the two satellites over the same area. Additionally, it is evident that the year 2022 exhibits reduced data availability not only in the northern east area but also in the central and eastern part of the region. All of these factors have led to the decision to utilize the gap-filled products for subsequent analyses. In this manner, there is the assurance of having continuous data throughout the year, already corrected for detection errors. When performing operations on this data, the use of non-optimized products could lead to the propagation of these errors, thereby resulting in inaccurate analyses.

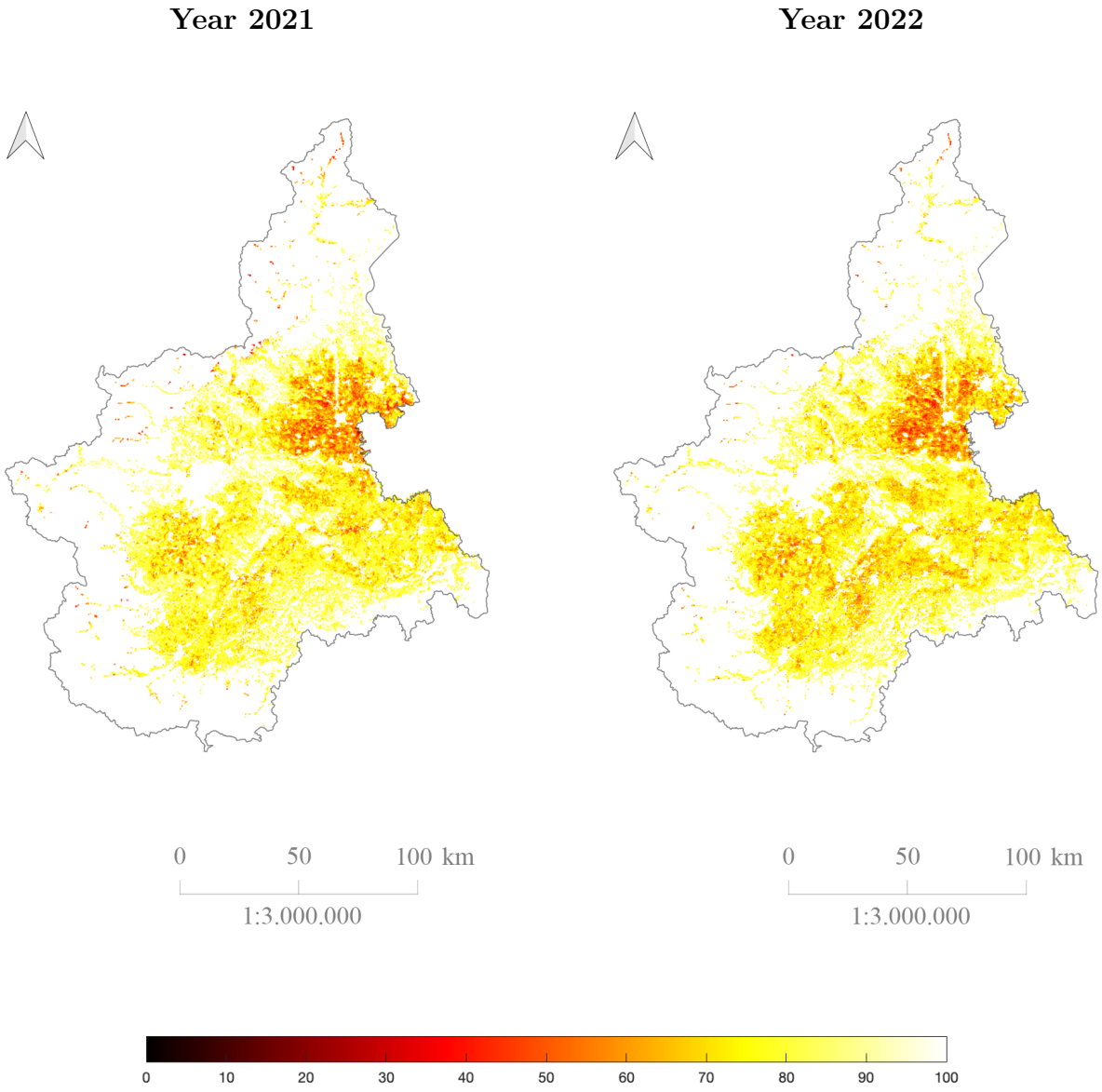

Figure 4.3: Availability analysis of data acquired by TERRA satellite for the years 2021 and 2022

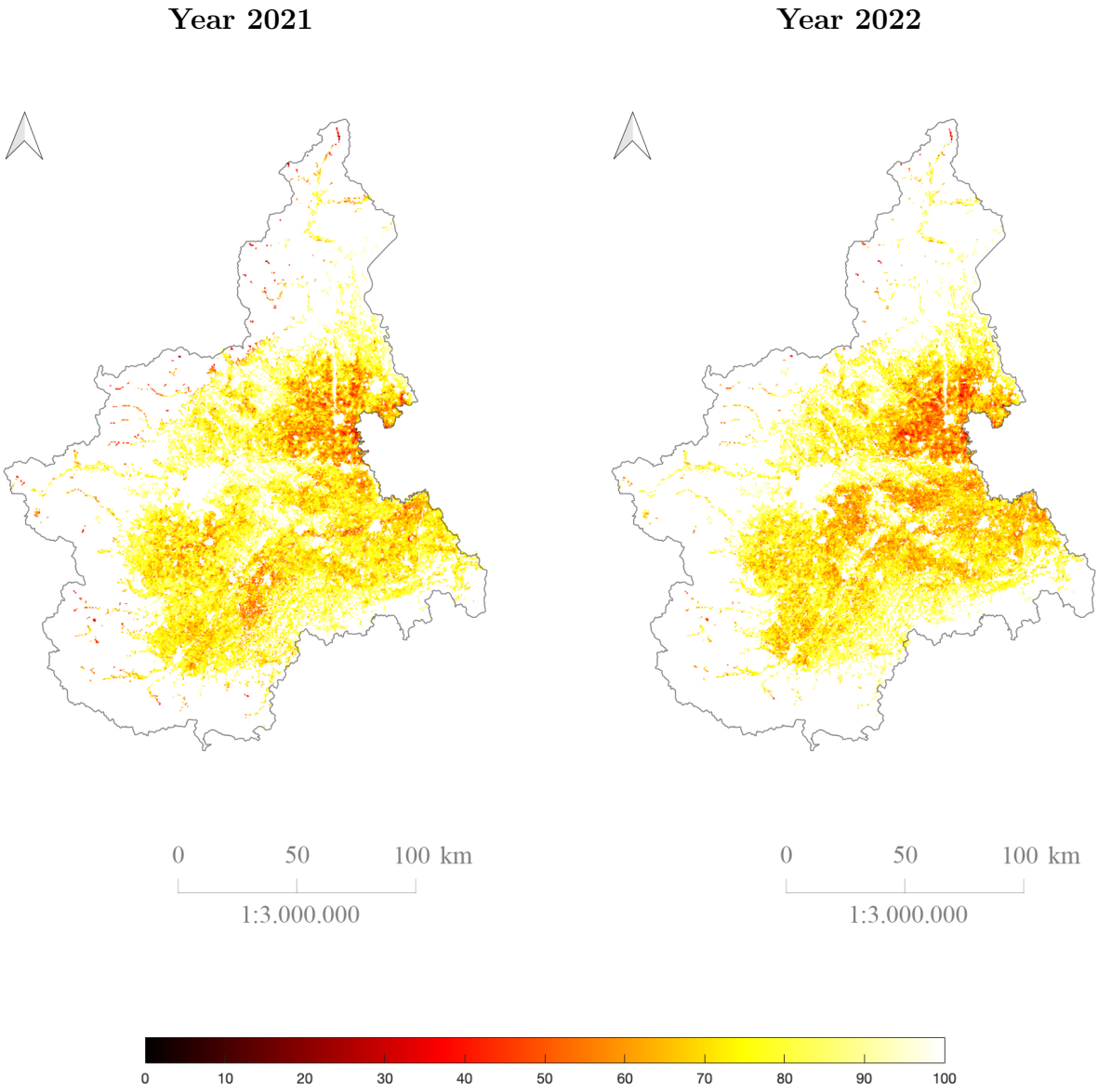

Figure 4.4: Availability analysis of data acquired by AQUA satellite for the years 2021 and 2022

In the next pages the results of the regional analysis of agricultural areas are displayed. As previously mentioned, the years under analysis encompass the biennium 2021 and 2022, and only data from optimized satellite products have been utilized.
In order to assess water stress in agricultural areas at the regional level, the average values of ET (Evapotranspiration) and PET (Potential Evapotranspiration) were calculated during the summer months. This period corresponds to when most seasonal crops are typically cultivated. The selected timeframe is based on previous studies [27] and was approximated according to the MODIS calendar. Indeed, the period considered in previous studies spans from May 15th to October 1st, lasting for 140 days, which coincides with the maize growing season, according to FAP [10]. Rounding this period to the MODIS calendar, which has an 8-day interval, the analysis begins on May 17th and concludes on October 7th of each year.
The results obtained from the ET data are presented in Figures 4.7-4.10. No significant differences are observed between the two satellite products, which, for both years, show similar values both numerically and spatially. It is evident that the southeast area of Piedmont is characterized by evapotranspiration values below the regional average. This pattern is consistent in both years and with both satellite products. The results for this area, located in the province of Alessandria, do not align with expectations. In fact, being a plain area and thus highly cultivated, higher ET values were expected compared to the rest of the region. From the maps, an ET estimate of approximately 10/15 mm per 8 days in the Alessandria area can be derived. Based on this rough estimate, it is straightforward to calculate a daily average ET of 1.25/1.9 mm/day, which is a low value for the considered season and location. Indeed, typical ET values for the summer season range from 3 to 7 mm/day. When observing other areas in Piedmont, an average ET of 22-28 mm/day is noticeable, which is reasonable and in line with expectations. It is also interesting to note that in areas closer to the mountains, ET values are higher compared to the plain and hill regions. This difference could be attributed to the types of crops grown in these areas. In fact, these regions typically have orchards, which are perennial and characterized by much higher ET rates.
It is possible that there may have been issues in the data collection process. Therefore, potential evapotranspiration data were analyzed using the same procedure described before. When dealing with potential evapotranspiration, the soil water content is not a limiting factor and depends only on climatic parameters. It is independent of crops and cultivation techniques, and serves as a measure of the soil water demand. The results are shown in the Figures 4.7, 4.8 and are in line with expectations. The plain areas, which are predominantly cultivated, are characterized by higher PET values. Going up in altitude and approaches the mountains, which are less cultivated, PET decreases, with minimum values of approximately

30 mm/8day. Looking at the figures, it can be observed that there are no differences between data collected by the TERRA and AQUA satellites in this case as well. However, differences between the years 2021 and 2022 are evident. The year 2021 is characterized by lower PET values compared to 2022, affecting all agricultural areas in the region, both in the plains and in the mountains. This substantial difference can be attributed to the high temperatures and limited rainfall that occurred during 2022. While this aspect may not be as evident in the ET maps, it becomes clear in the analysis of PET, as it represents the soil and crop water demand.
In order to comprehensively evaluate the MODIS satellite product and determine whether values below the average ET indicate water stress or not, a local-scale study is necessary.

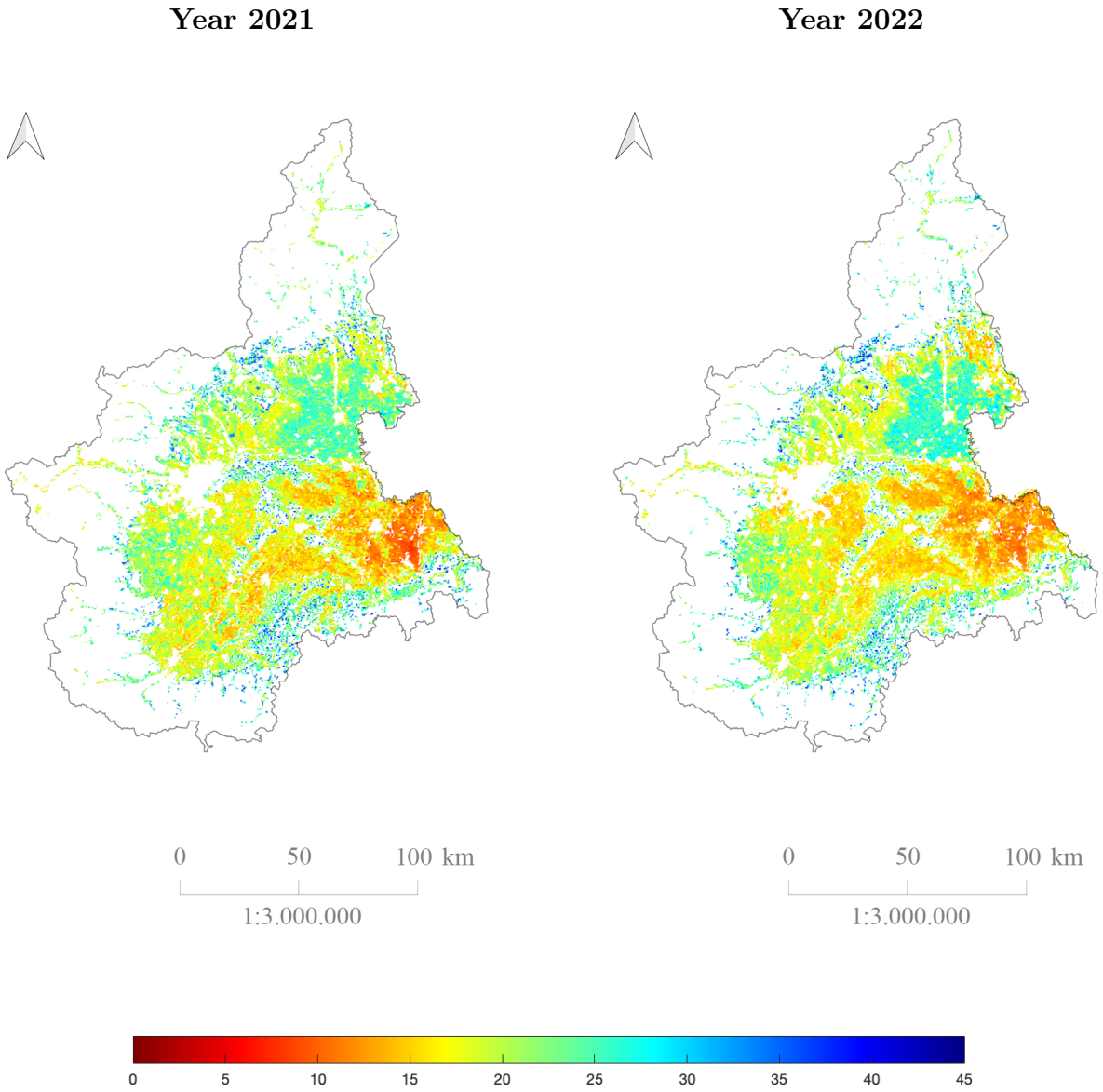

Figure 4.5: Evapotranspiration analysis of data acquired by TERRA satellite for the years 2021 and 2022

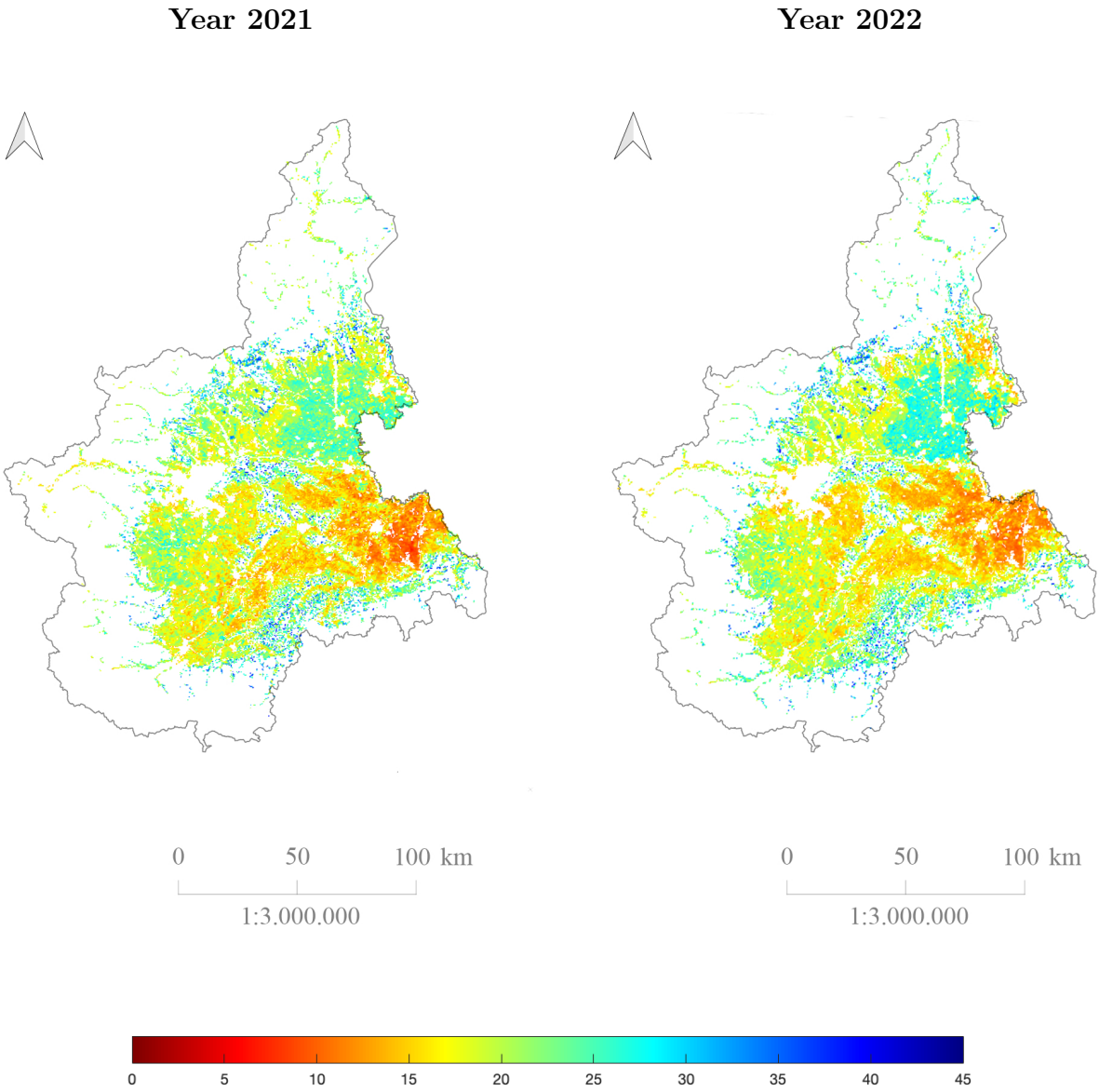

Figure 4.6: Evapotranspiration analysis of data acquired by AQUA satellite for the years 2021 and 2022

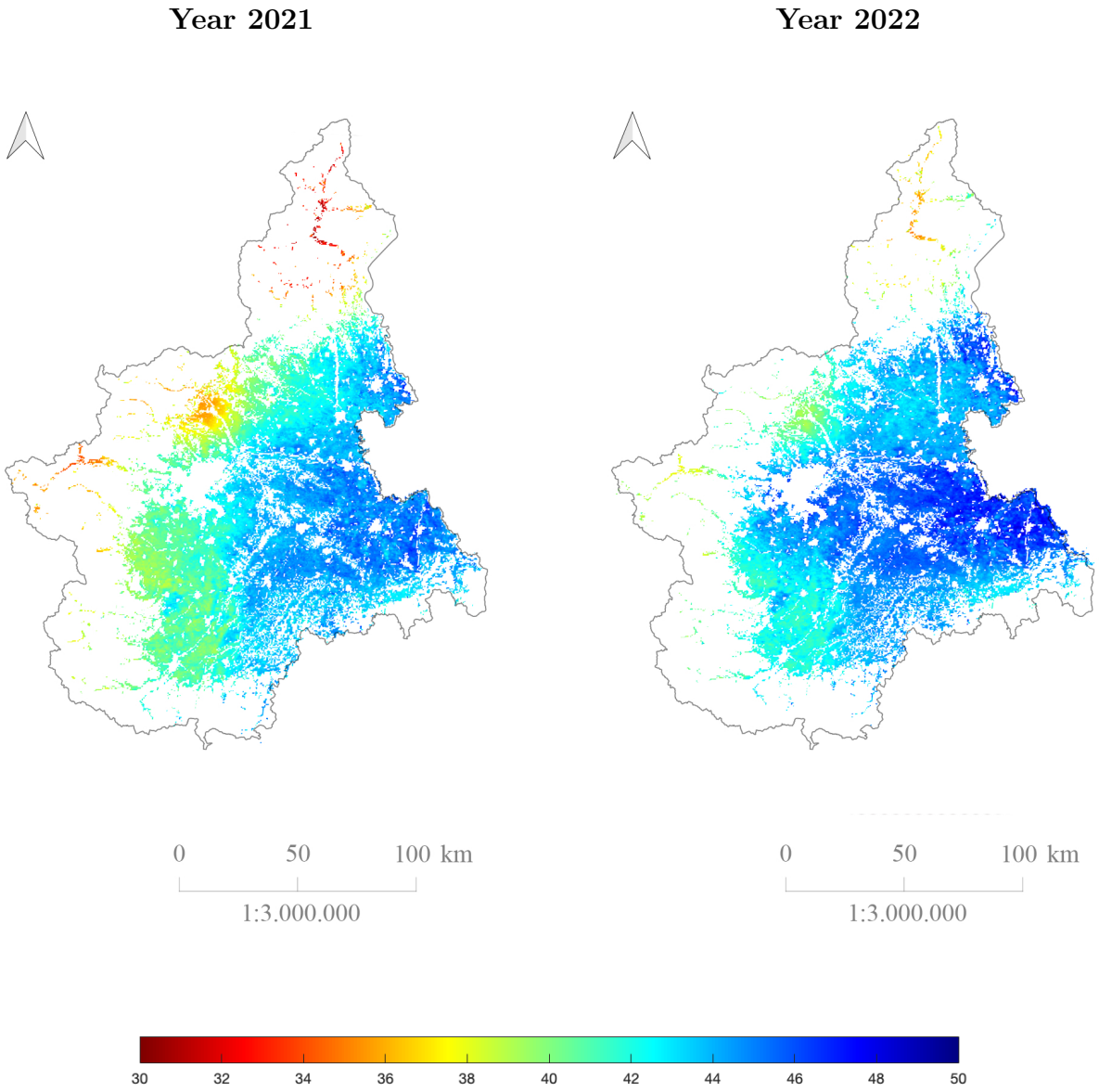

Figure 4.7: Potential evapotranspiration analysis of data acquired by TERRA satellite for the years 2021 and 2022

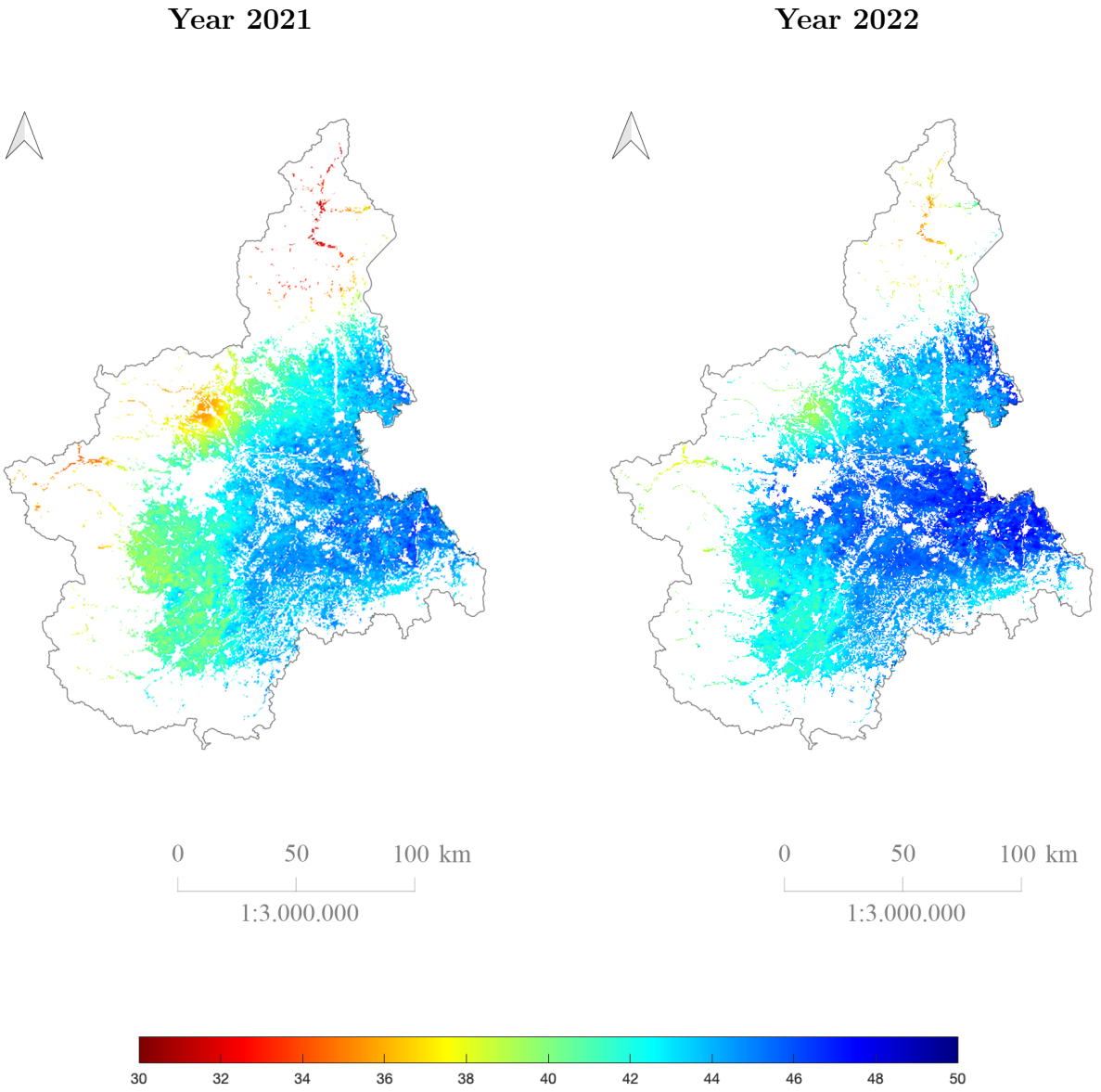

Figure 4.8: Evapotranspiration analysis of data acquired by AQUA satellite for the years 2021 and 2022

4.4 Local analysis of maize fields

4.4.1 Turin

For this initial local analysis, two single-crop cultivated areas in the province of Turin are under consideration. The areas encompassed within the province are depicted in Figure 4.9. In particular, the two selected areas are located in the Caluso and Montanaro districts (Figure 4.10), within the Canavese region. Agriculture in these areas predominantly consists of grains and grapevines, which are cultivated on both hilly and plain terrain.
According with the *Anagrafe Agricola* by Regione Piemonte, the selected areas are uniformly cultivated with maize both on 2021 and 2022, as it can be seen from Figures 4.12, 4.13, 4.14, 4.15. In 2021, although some fields within the designated areas were cultivated with different crops, these represent a small percentage in comparison to the entire area. Therefore, the two areas can still be uniformly classified as maize-cultivated.

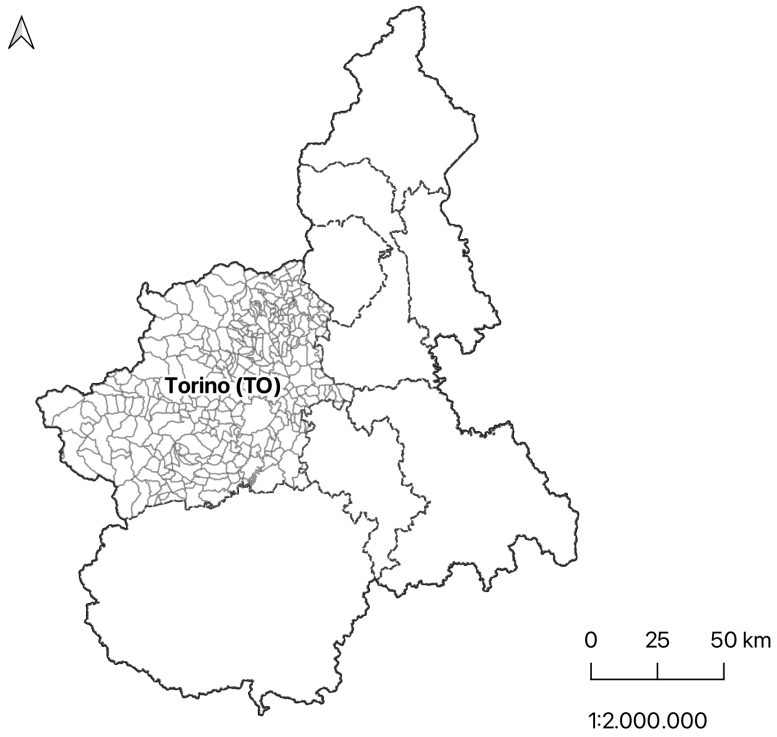

Figure 4.9: Province of Turin

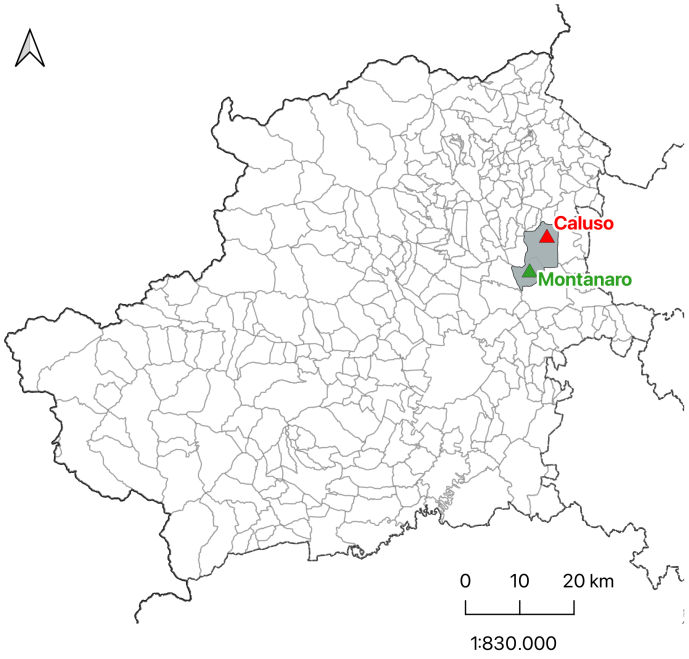

Figure 4.10: Caluso and Montanaro districts

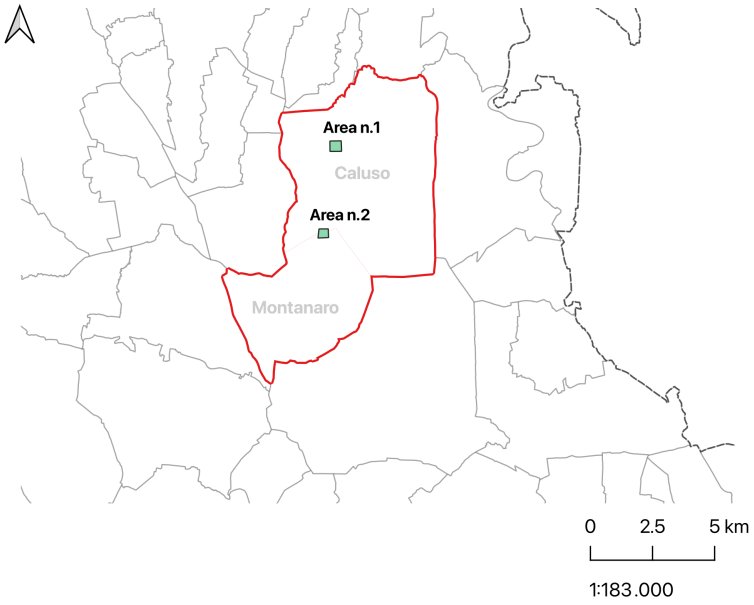

Figure 4.11: Location of the two studied areas, Turin

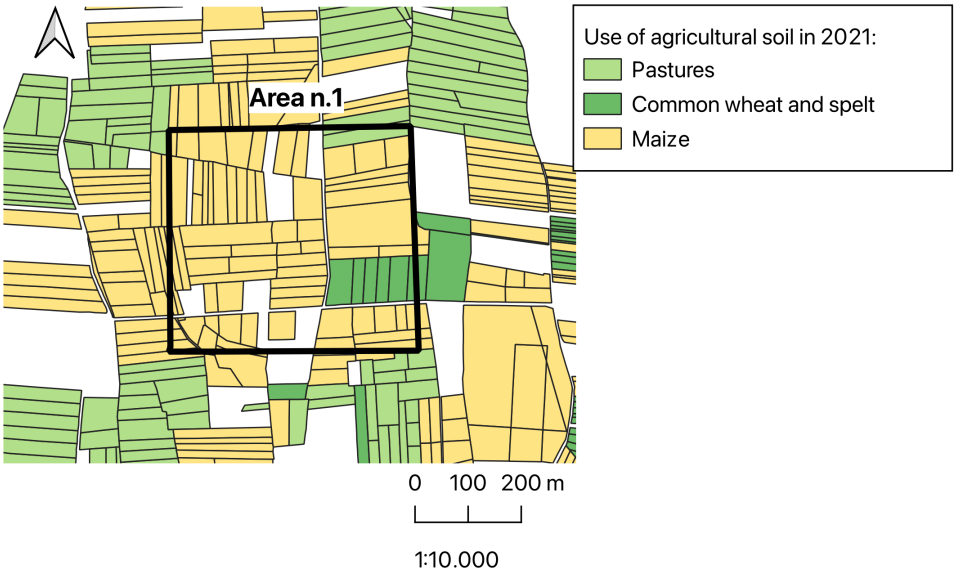

Figure 4.12: Use of agricultural soil in Area 1 for the year 2021

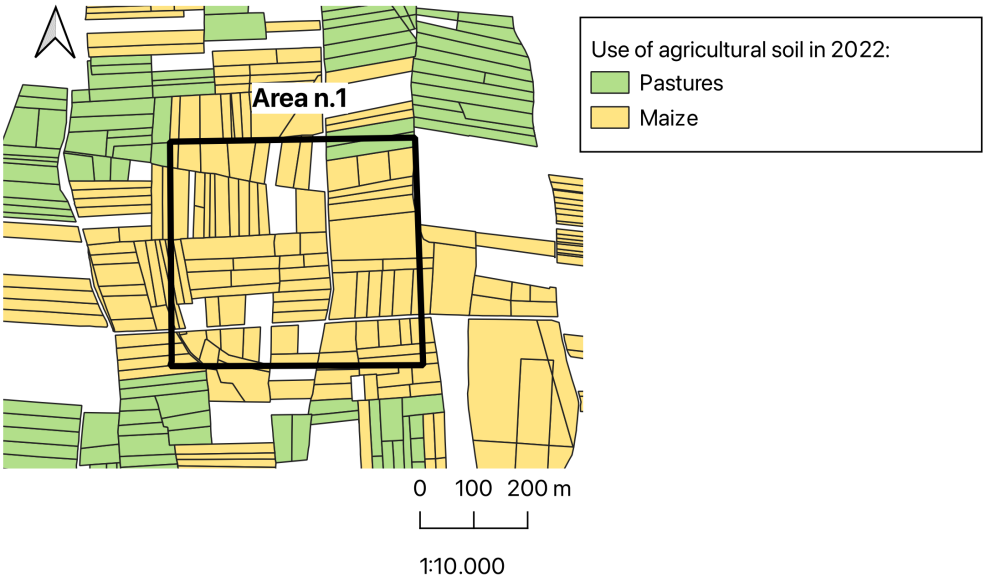

Figure 4.13: Use of agricultural soil in Area 1 for the year 2022

Figure 4.14: Use of agricultural soil in Area 2 for the year 2021

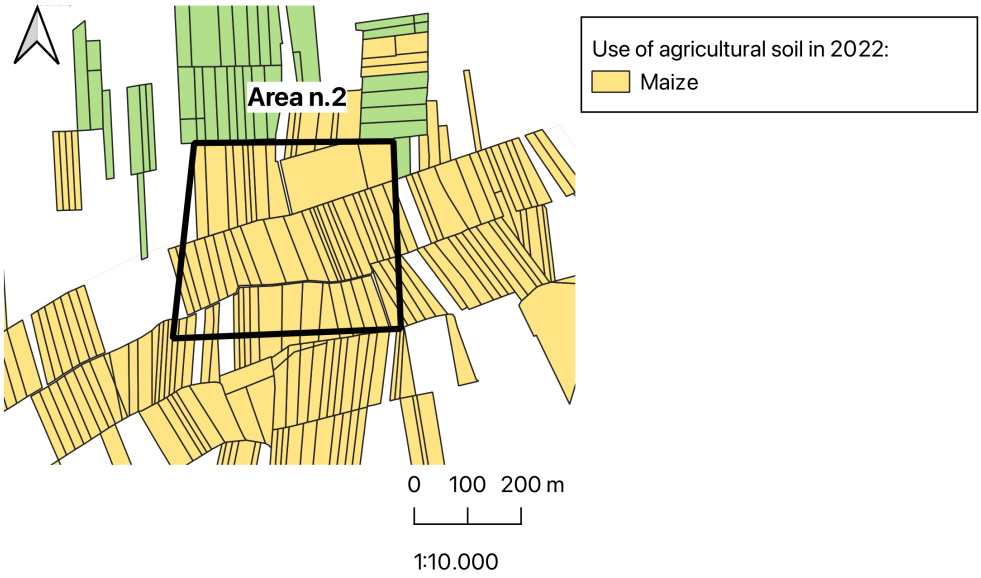

Figure 4.15: Use of agricultural soil in Area 2 for the year 2022

According to the Corine Land Cover 2018 classification, the identified areas are cultivated without the use of irrigation, under rainfed conditions. For this reason, a comparative analysis was conducted between the hydrological model under rainfed conditions and MODIS satellite data.

For this analysis, the meteorological data were taken from ground station data-set provided by Arpa. In this case, the Caluso weather station, located 2 km and 5 km away from areas 1 and 2, respectively, was used. The results are displayed in the following figures. In each plot, the trends of ET and PET recorded by the MODIS satellite, as well as the estimation of ET_0 and ET calculated using the mathematical model, were depicted. The x-axis corresponds to the day of the year under consideration, while the y-axis represents the evapotranspiration values expressed in millimeters of water over an 8-day period. The sowing and harvest dates are also indicated in order to emphasize the period under study. Clearly, the estimation of ET ed ET_0 by means of the hydrological model encompasses only the crop's growth period.

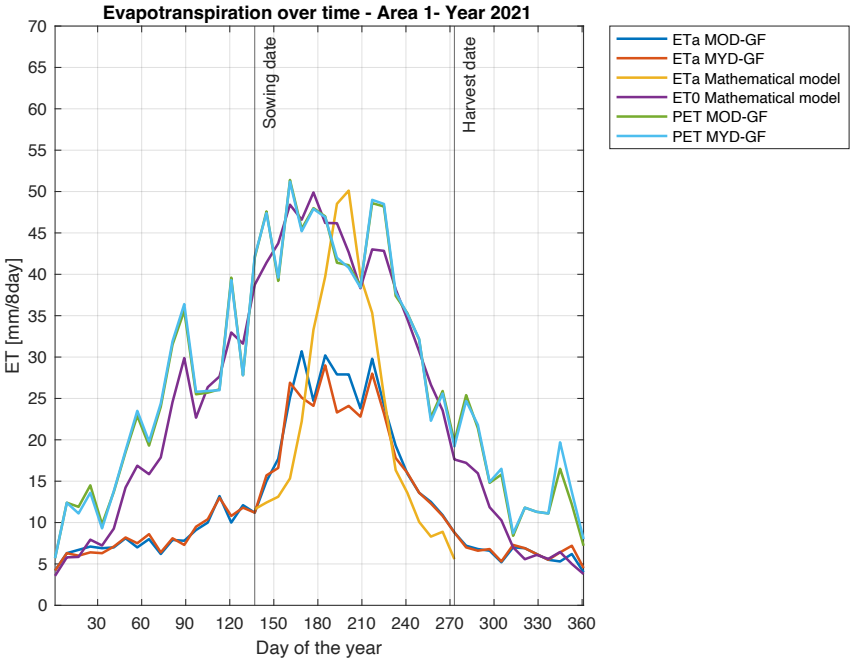

Figure 4.16: Evapotranspiration trend during 2021, Area 1 Turin

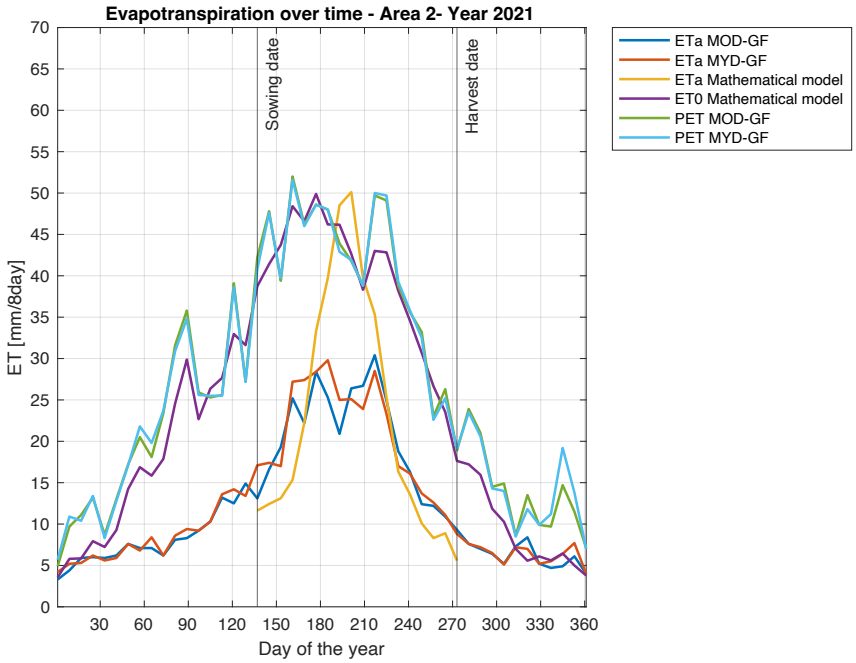

Figure 4.17: Evapotranspiration trend during 2021, Area 2 Turin

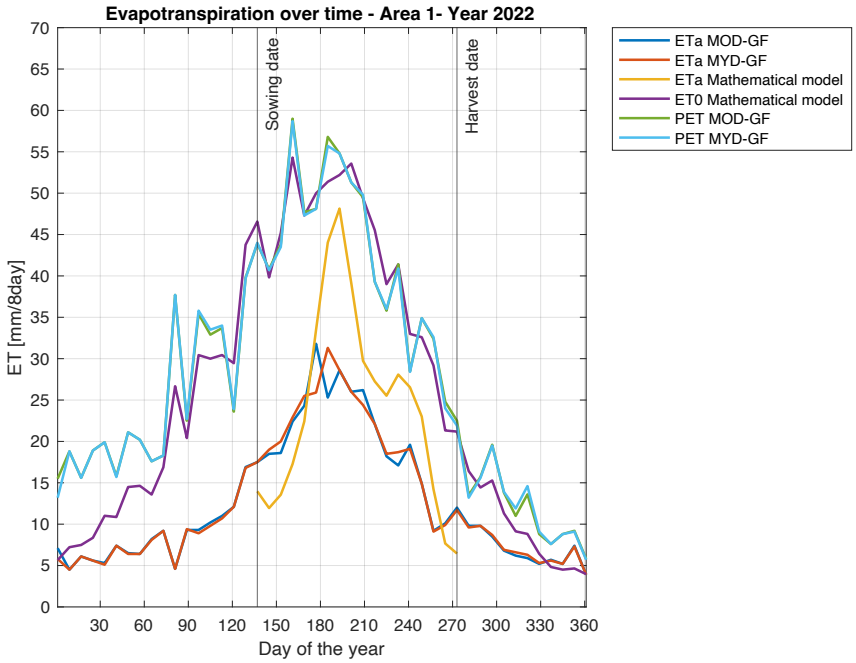

Figure 4.18: Evapotranspiration trend during 2022, Area 1 Turin

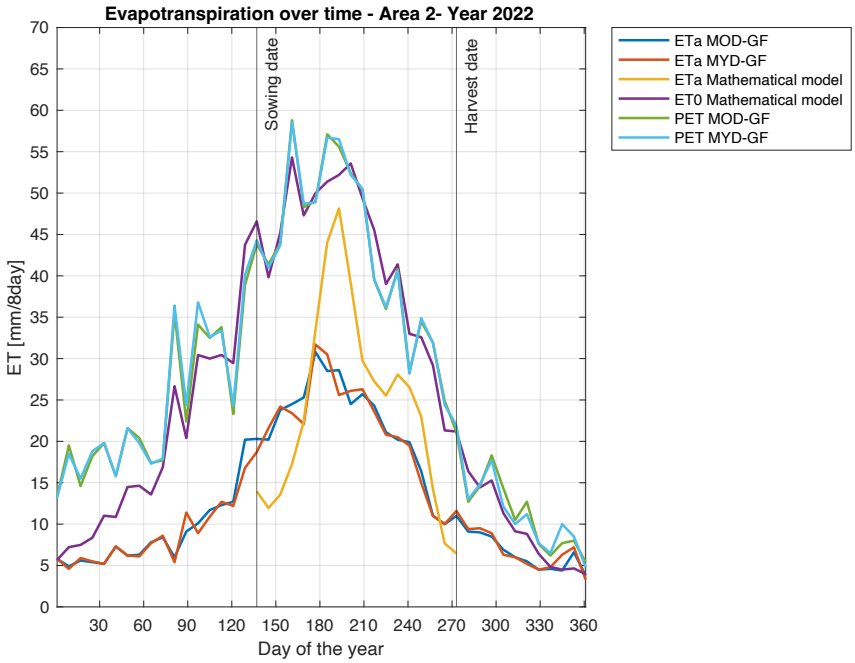

Figure 4.19: Evapotranspiration trend during 2022, Area 2 Turin

Regarding the satellite data acquired by the two satellites AQUA and TERRA, these are comparable. They both show similar trends throughout the year, with substantial overlap. In general, when considering all variables, two distinct trends can be observed in the two years.
In the year 2021, for both areas, satellite data recorded maximum values of PET equal to 50 mm/8day and ET equal to 30 mm/8days. A comparison with values estimated by the model highlights that ET_0 follows a similar pattern to PET both during the maize growth period and the remaining days of the year. The annual trend compared to the expected one shows minimum values during the winter season and maximum values during the summer season. However, there is a significant discrepancy in ET values. This difference occurs during the intermediate stage of plant development, where actual evapotranspiration exceeds the potential evapotranspiration measured by the satellite.
In the year 2022, the recorded satellite values for PET and ET are higher compared to the previous year, with maximum values of 58 mm/8days and 32 mm/8days. The ET_0 and PET trends are similar in this case as well, with a misalignment in the early part of the year. MODIS data, however, detect higher PET values, approximately three times those modeled. This may be due to an error during satellite detection or a lack of data caused by cloud cover during this time of year. The use of gap-filled products, which involve interpolation to compensate

for missing data, can lead to erroneous estimates if the missing data correspond to a relatively long period (on the order of weeks). ET values in 2022 exhibit a more pronounced mismatch compared to 2021. In the initial phase of plant growth, the model estimates lower ET compared to satellite data and then overestimates it from the development phase to the late stage. In this year, the model's ET estimate does not reach the PET values, remaining below them.
The performance of the MODIS product compared to the model was then analyzed. To achieve this, an investigation was conducted to verify the presence of a potential correlation between satellite data and modeled data through their representation in a scatter plot. The x-axes corresponds to the ratio between ET and PET acquired by the satellite, while on the y-axes the ratio between actual ET and reference ET estimated by the model. The results are displayed below and they refer to maize growing period.

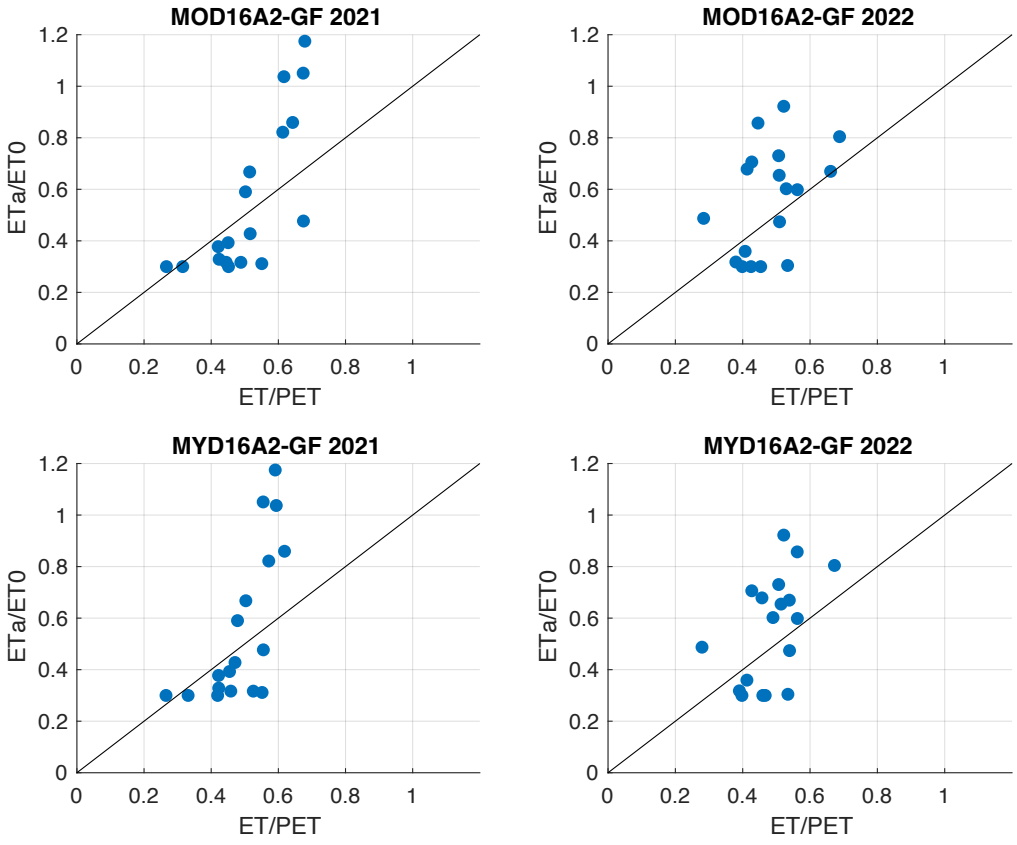

Figure 4.20: Scatter plots of modelled and satellite data over Area 1, Turin

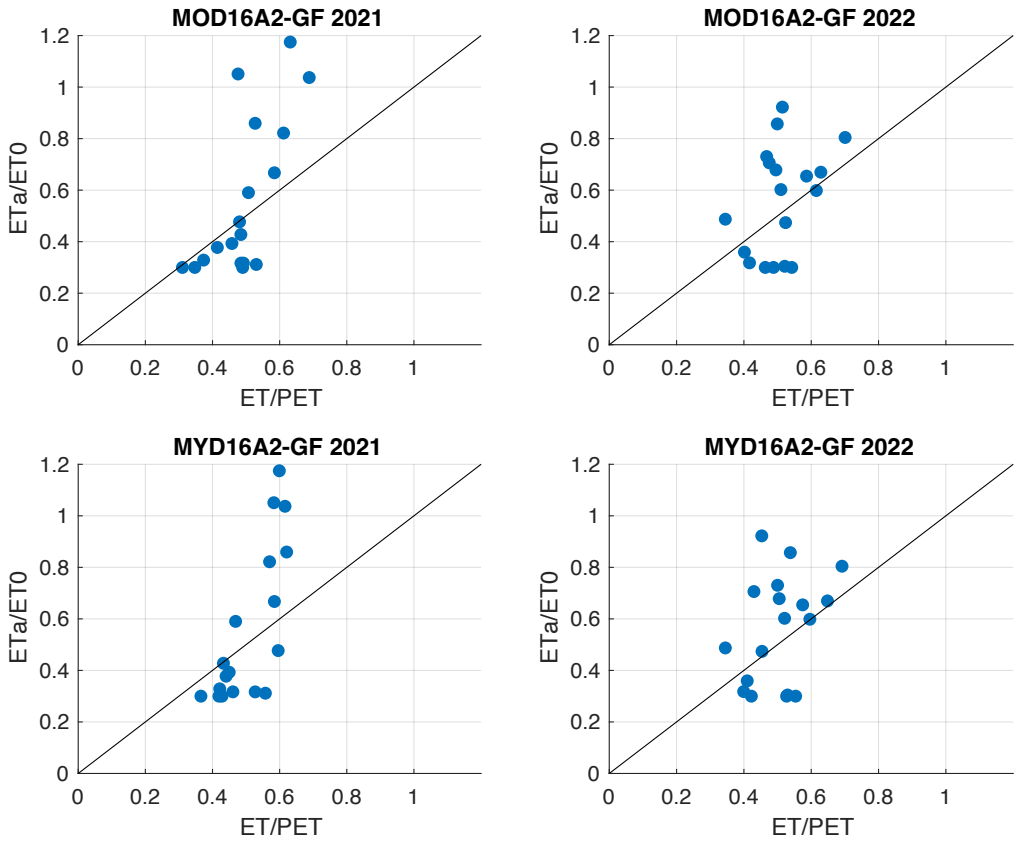

Figure 4.21: Scatter plots of modelled and satellite data over Area 2, Turin

As can be observed, it is not possible to identify any kind of correlation between the two types of data, with the exception of a few values. The scatter plots confirm that the model's ET estimate is consistently higher than that of MODIS, reaching a factor of 2 in some cases.
A possible cause of the mismatch between the modelled and satellite data can be attributed to the different meteorological input parameters, in particular precipitation data. Indeed, the meteorological data used as input for the model come from a weather station nearby. Although the distance from the weather station to the fields is not significant, there can be slight variations in precipitation data. It is possible that the weather station recorded rainfall events that did not actually occur at the fields location. This could explain the model's overestimation of ET compared to satellite data, which might result from an overestimation of available soil moisture.

4.4.2 Alessandria

For this second local analysis, an area located in the Alessandria province is considered. The area encompassed within the province are shown in Figure 4.22. Also in this case, the selected area is a single-crop cultivated field which is located in the Alessandria district 4.23. The region is predominantly plain, where the primary cultivated crops are cereals, such as wheat, barley, maize, soybeans, and sunflowers.
According with the *Anagrafe Agricola* by Regione Piemonte, the area under study is uniformly cultivated with maize both on 2021 and 2022, as it can be seen from Figures .

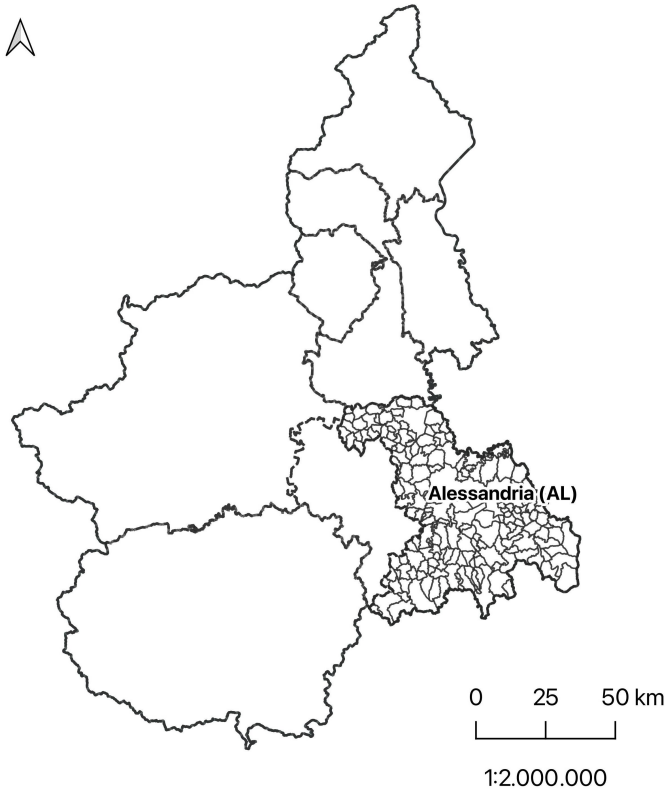

Figure 4.22: Province of Alessandria

Figure 4.23: Location of the studied area, Alessandria

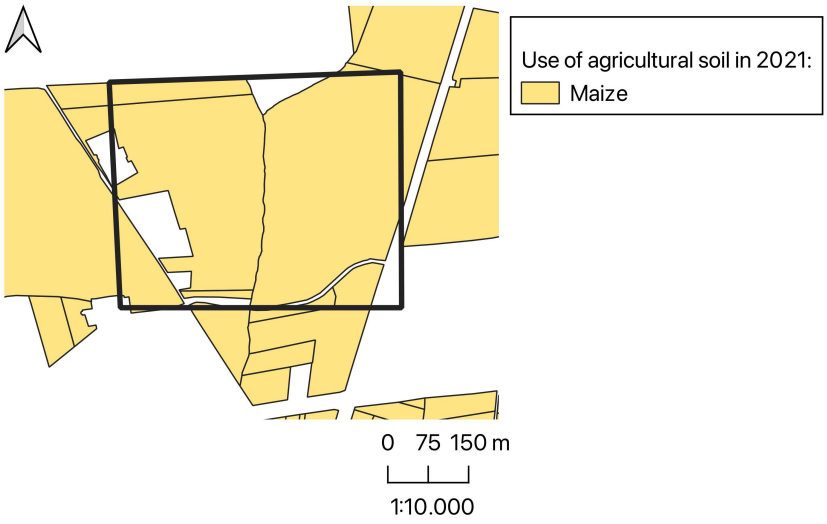

Figure 4.24: Use of agricultural soil in 2021 for the area under study in Alessandria

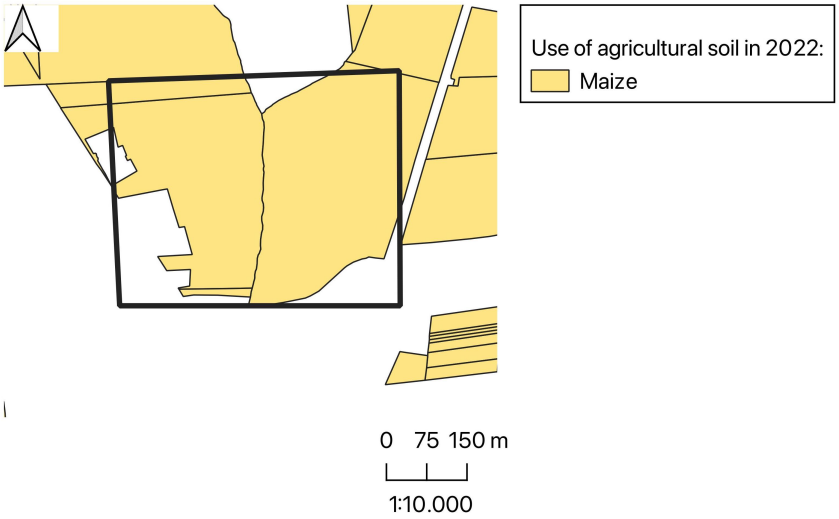

Figure 4.25: Use of agricultural soil in 2022 for the area under study in Alessandria

According to the Corine Land Cover 2018 classification, the identified areas are cultivated without the use of irrigation, under rainfed conditions. For this reason, a comparative analysis was conducted between the hydrological model under rainfed conditions and MODIS satellite data. For this analysis, the meteorological data used are taken from the gridded data-set provided by Arpa. Thus, the temperature and precipitation data input into the model derived from the interpolation of nearby ground-stations data and are specific to the considered field.
The results are displayed in Figures 4.26, 4.27. In each plot, the trends of ET and PET recorded by the MODIS satellite, as well as the estimation of ET_0 and ET calculated using the mathematical model, were depicted. The x-axis corresponds to the day of the year under consideration, while the y-axis represents the evapotranspiration values expressed in millimeters of water over an 8-day period. The sowing and harvest dates are also indicated in order to emphasize the period under study. Clearly, the estimation of ET ed ET_0 by means of the hydrological model encompasses only the crop's growth period.
Also in this case, satellite data acquired by the AQUA and TERRA platforms are comparable. They both show similar trends throughout the year, with a total overlap of PET values. Concerning ET values, the two satellite data exhibit a similar behaviour during 2021 while a less matching during the growing period is observed. These values have different peaks between days 100 and 210 of the year 2022, ranging between 10 and 17 mm/8day.

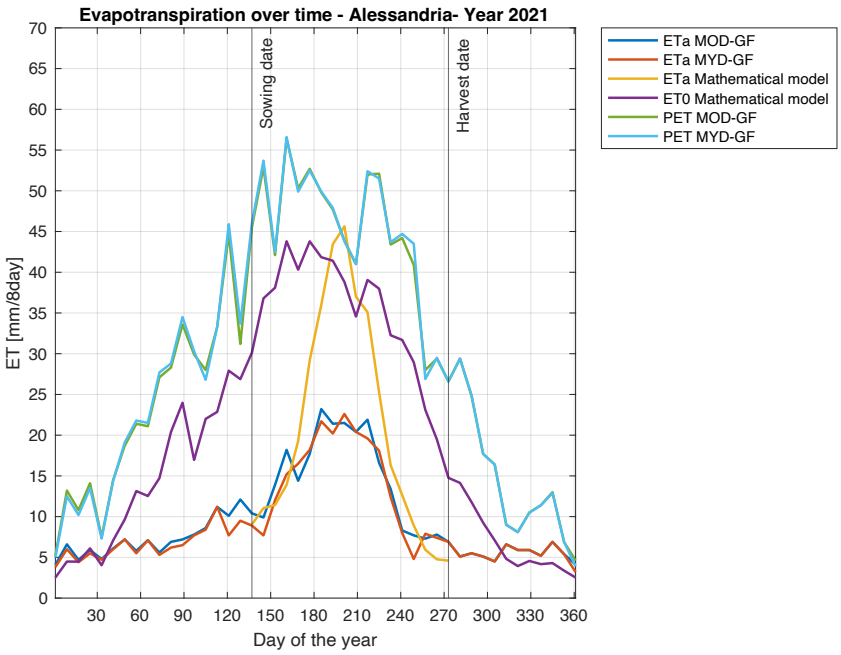

Figure 4.26: Evaporation trend during 2021, Alessandria

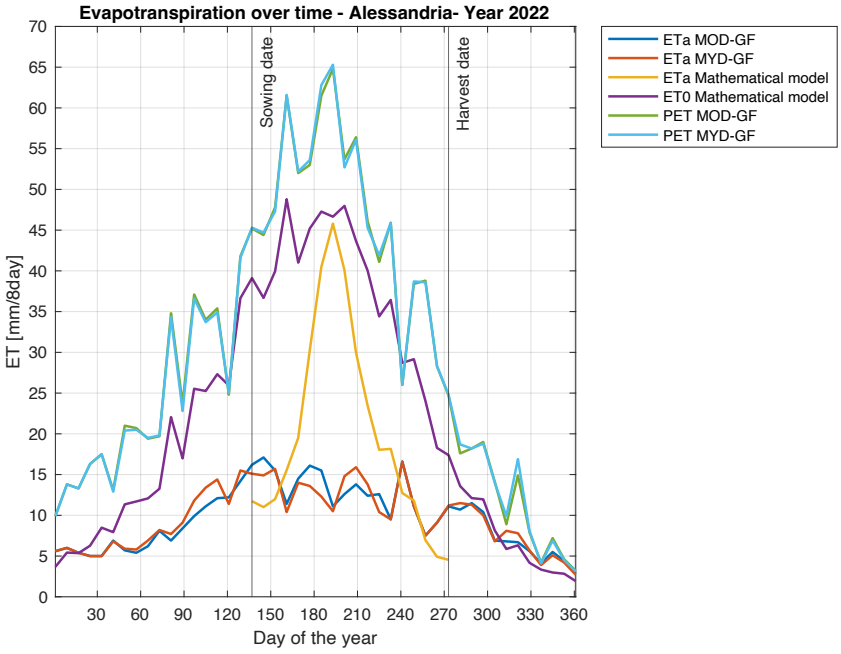

Figure 4.27: Evaporation trend during 2022, Alessandria

By looking at the plots, two distinct trends can be observed between 2021 and 2022. In 2021, the maximum PET value reaches 56 mm/8day while maximum ET values are equal to 23 mm/8day. The behaviour of ET_0 estimated by means of the mathematical model is similar to the one of PET throughout the year but with lower values, reaching peaks of 44 mm/8day. The annual trend, compared to the expected one, shows minimum values during the winter season and maximum values in the summer period. Also in this case, as the previous one of Turin, a significant mismatching is observed between satellite ET data and the modelled ones.This difference occurs during the intermediate stage of plant development, where actual evapotranspiration reaches the potential evapotranspiration measured by the satellite. In this year, it can also be noticed a shift in the peak of PET towards the early stage of the crop's growing period. This shift is also observed in the ET_0 trend.
Regarding the year 2022, the recorded satellite PET values are higher compared to the previous year, with maximum values of 65 mm/8days. The ET_0 and PET trends are similar in this case as well, with a misalignment in the early part of the year. As in the previous case of Turin, this may be due to an error during satellite detection or a lack of data caused by cloud cover during this time of year. The recorded PET values by the satellite are approximately two times those modeled. In the year 2022, evapotranspiration values are affected by a strong discrepancy between satellite and modelled data. This mismatch is present over the entire growing period, with a little exception in the last part of the period. MODIS evapotranspration data are significantly low for the summer season, with values of 10 mm/8day during crop development stage. These values confirm what was observed during the regional-scale analysis and translate to a daily evapotranspiration rate of 1.25 mm/day. Observing what has been modeled, the values are not comparable. The model's ET, in fact, reaches values of 45 mm/8 days, which is equivalent to 5-6 mm/day. These are the values expected from a summer crop during its maximum vegetative phase. In this case, the model's ET estimate does not reach the PET values, remaining below them.
Then, the performance of the MODIS product compared to the model is analyzed. To achieve this, an investigation is conducted to verify the presence of a potential correlation between satellite data and modeled data through their representation in a scatter plot. The x-axes corresponds to the ratio between ET and PET acquired by the satellite, while on the y-axes the ratio between actual ET and reference ET estimated by the model. The results are displayed in Figure 4.28 and they refer to maize growing period.
As it can be noticed, it is not possible to observe any correlation between the two types of data, with the exception of few values in 2021. The scatter plots confirms also in this analysis that the modelled ET estimations is significantly higher than those of MODIS, reaching a factor 2 in some cases.

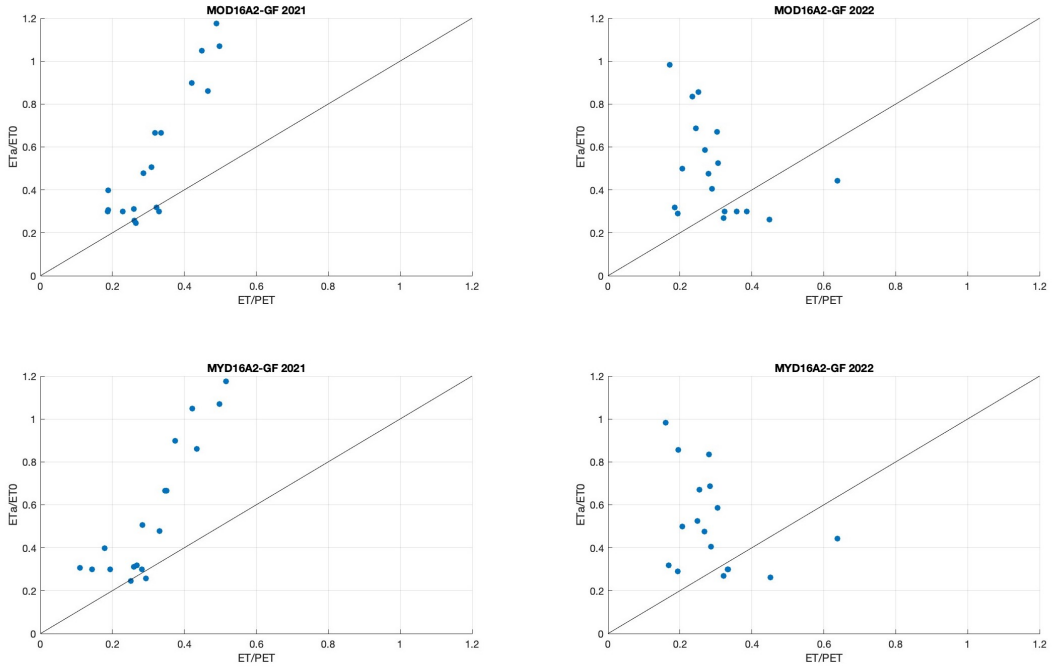

Figure 4.28: Scatter plots of modelled and satellite data, Alessandria

Since, in this case, the meteorological inputs refer to the specif location of the field, a further analysis of these inputs is carried out. Specifically, a comparison between gridded data and ground-based data from the nearest weather station is performed. Daily temperature and precipitation data from the station of San Salvatore (AL) are taken, which distances 5.5 km from the field under study. In this way, it is possible to verify if there are differences in the meteorological inputs that are then reflected in the ET estimation.
Regarding temperature data, the minimum and maximum values representing meteorological inputs of the model have been plotted in scatter plots (4.29). On the x-axis the temperature values from meteorological stations are displayed, while on the y-axis the values from the gridded data-set are represented.
In general, the data are well correlated with each other and do not exhibit significant differences. The minimum temperature data show a stronger correlation compared to the maximum temperature data, which display a slight deviation in 2022. Looking at figure (d), it is evident that the data recorded by the weather station are slightly higher than the gridded data derived from interpolation. However, this does not significantly affect the estimation of ET.

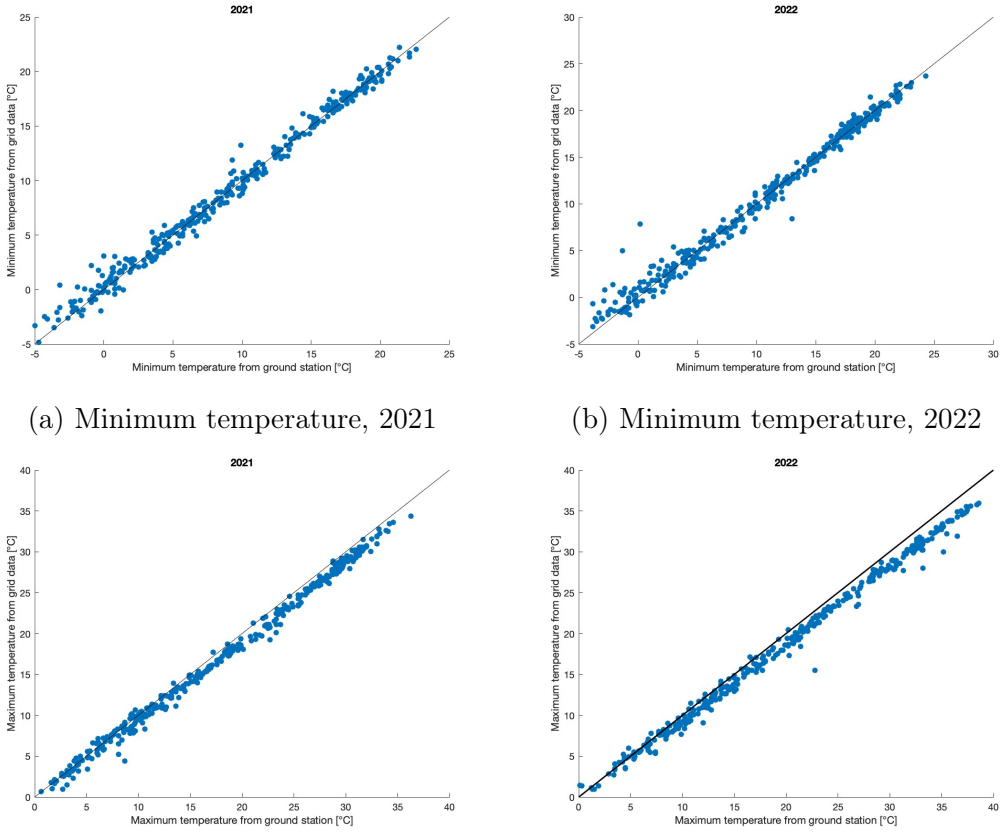

(a) Minimum temperature, 2021

(b) Minimum temperature, 2022

(c) Maximum temperature, 2021

(d) Maximum temperature, 2022

Figure 4.29: Scatter plots of minimum and maximum temperature, Alessandria

Regarding precipitation data, the volumes of rainfall and the number of rainy days are compared for each month of the year. In the latter case, a rainy day is defined as any day with a daily precipitation equal to or greater than 1 mm. The results are reported below, in Figures 4.30, 4.31, 4.32, 4.33.
The number of rainy days are overall comparable, with the exception of January, July and December months of the year 2021. Data of 2022 show a better correlation between grid and ground data throughout the entire year.
However, this discrepancy in the number of rainy days is vanished when observing the cumulative volumes of rainfall for each month. In fact, the data for 2021 show very similar values. Even in 2022, there is a good correlation between the volumes of rainfall, with the exception of the months of June and August, where the gridded data show significantly higher rainfall volumes compared to those measured by the weather station. The detection of higher precipitation in the gridded data is due to the interpolation of data measured by multiple nearby weather stations. Therefore,

the gridded data is influenced by several weather stations in the vicinity of the area of interest. Additionally, it is important to take into account that precipitation events can occur locally, affecting relatively small areas.
Furthermore, there is a notable difference both in the number of rainy days and in the volumes of water between the two years. The most significant difference is observed in the early months of the year. In 2021, there was a good amount of rainfall in the first months of the year, except for March when there was no rain. The situation is quite different in 2022, where barely 20 mm of rainfall per month were reached.

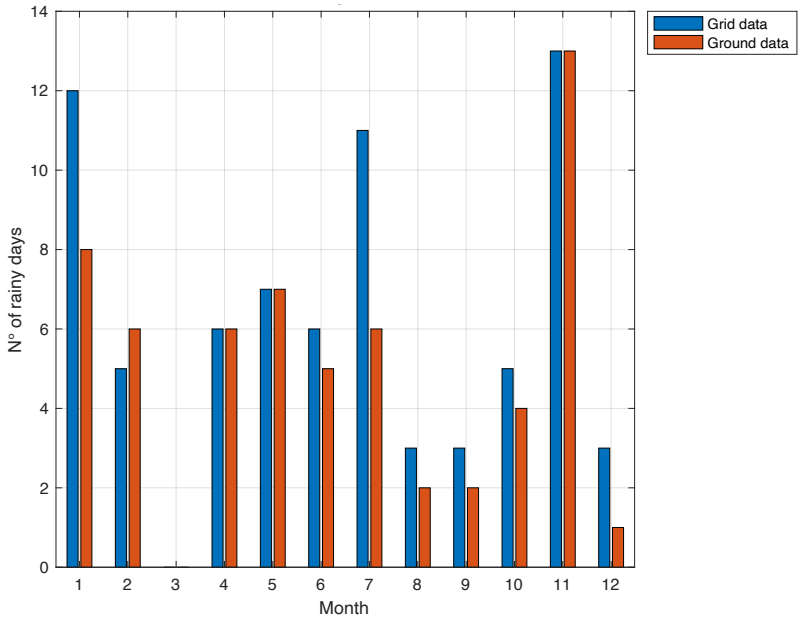

Figure 4.30: Number of rainy days per month, year 2021

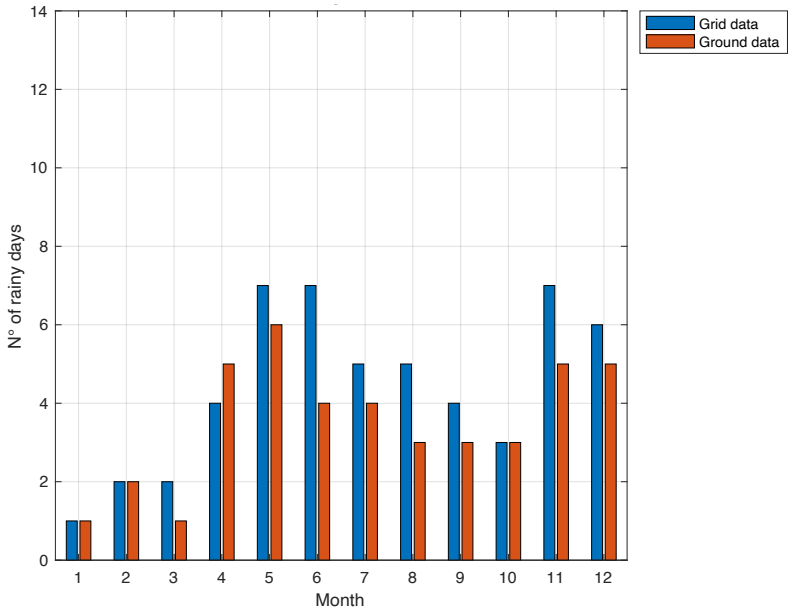

Figure 4.31: Number of rainy days per month, year 2022

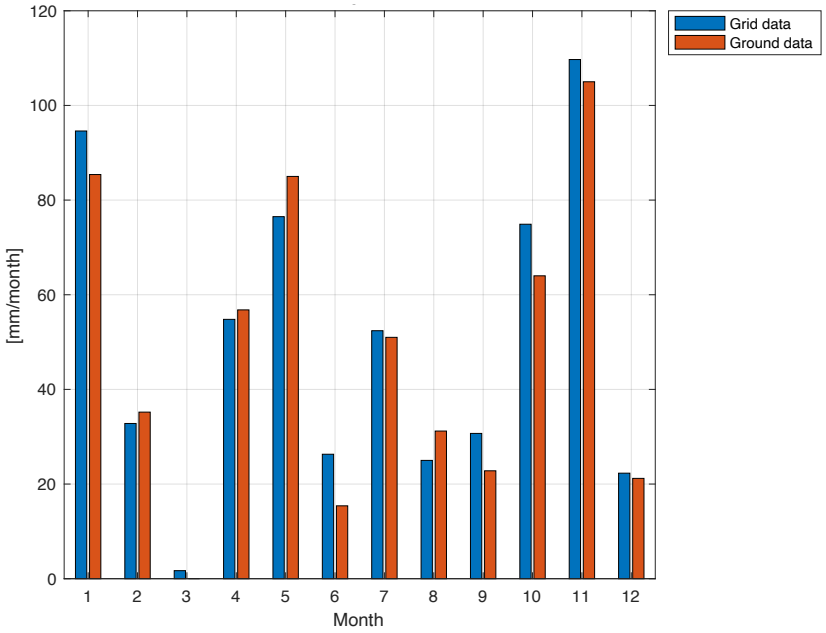

Figure 4.32: Volume of rainfall per month, year 2021

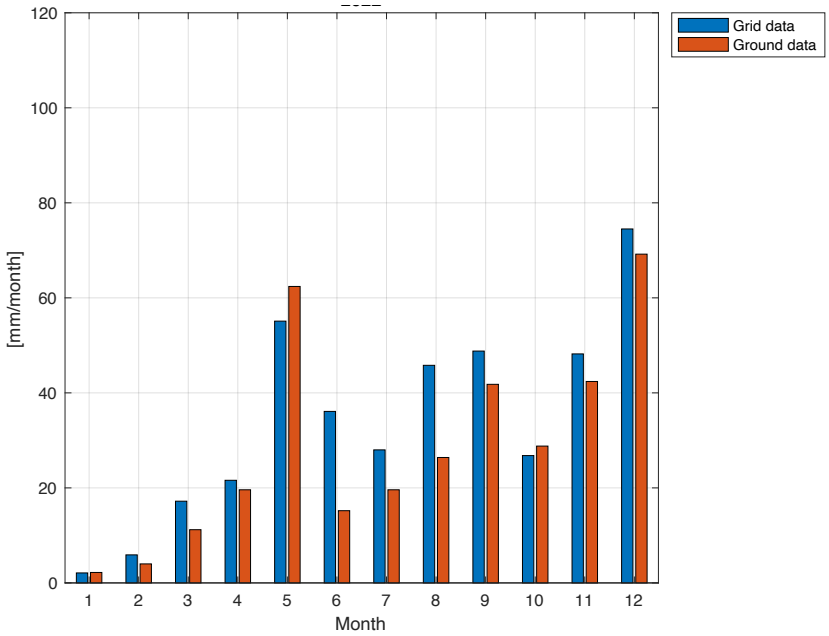

Figure 4.33: Volume of rainfall per month, year 2022

Since the Alessandria area has shown anomalous and underestimated values of evapotranspiration, the analysis to this region was extended to ten additional areas. Each area has dimensions of 500m x 500m and is located within the province of Alessandria (Figure 4.34).

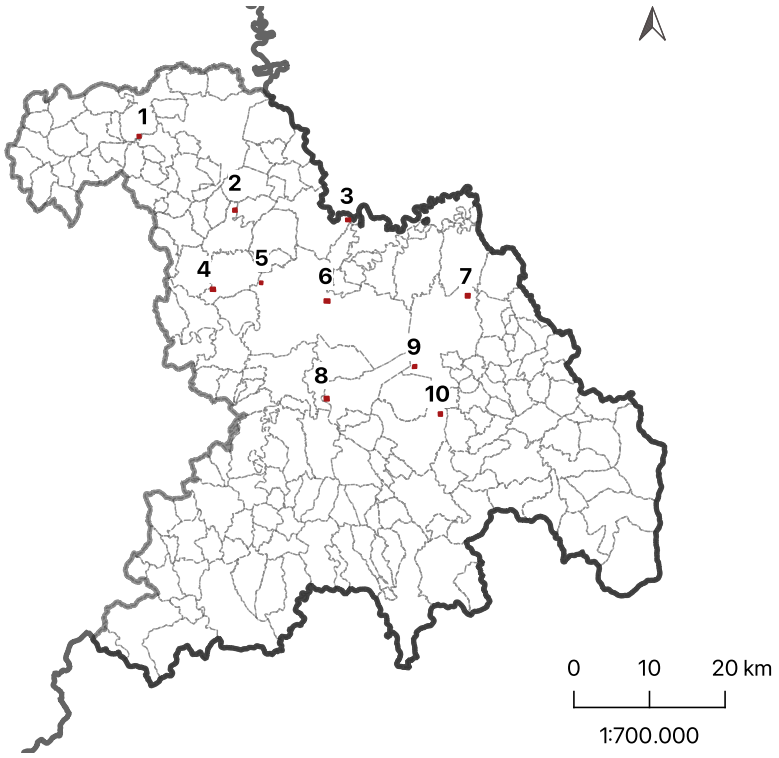

Figure 4.34: Location of the ten areas in the province of Alessandria

The areas considered are uniformly cultivated with maize in the year 2022 while most of these are cultivated with other crops in the year before. This choice was made because according to the *Anagrafe Agricola* by Regione Piemonte, many fields with the specified dimensions in this region are not uniformly cultivated with maize. Therefore, areas cultivated with maize were specifically sought for the year 2022, as it is the period that has shown uncertain values of evapotranspiration.
As for the previous analysis, the meteorological input data for the model were taken from the gridded data-set provided by ARPA Piemonte. The estimation with the mathematical model still refers to the maize growth period. The results obtained are displayed in the following figures.

Year 2021

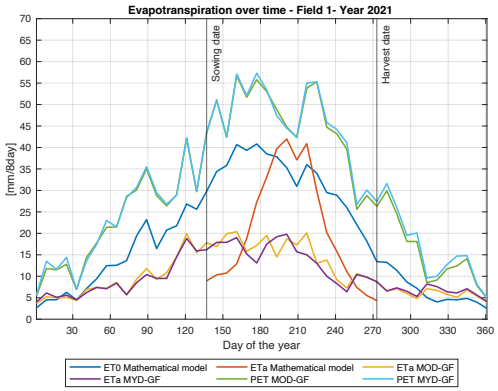

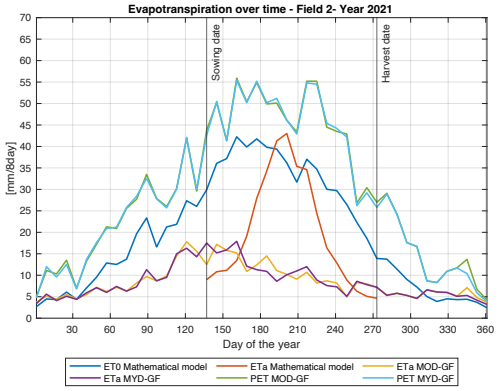

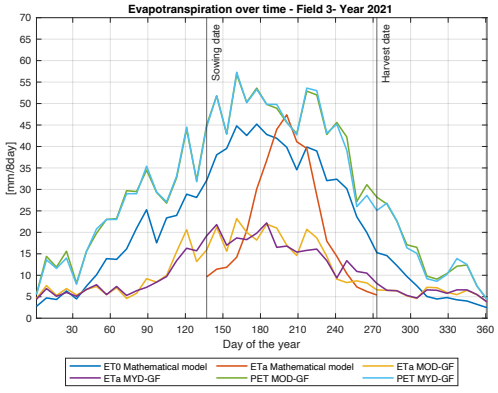

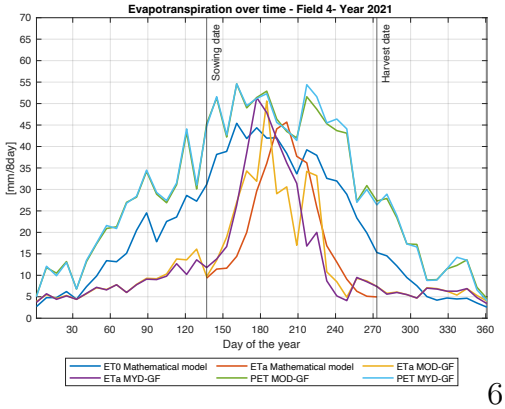

Year 2022

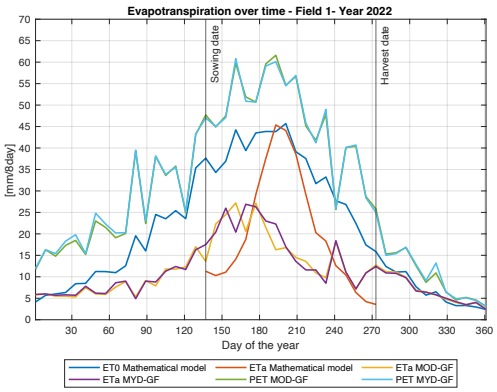

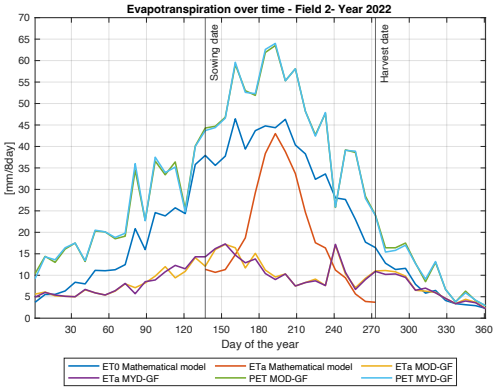

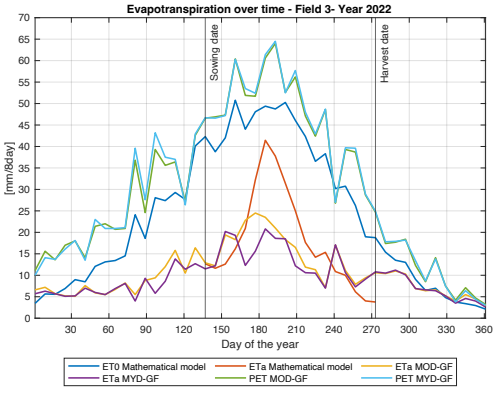

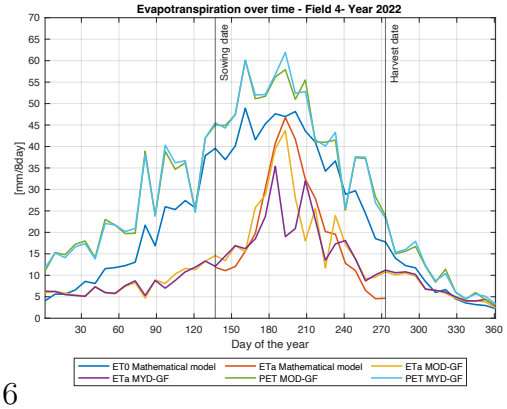

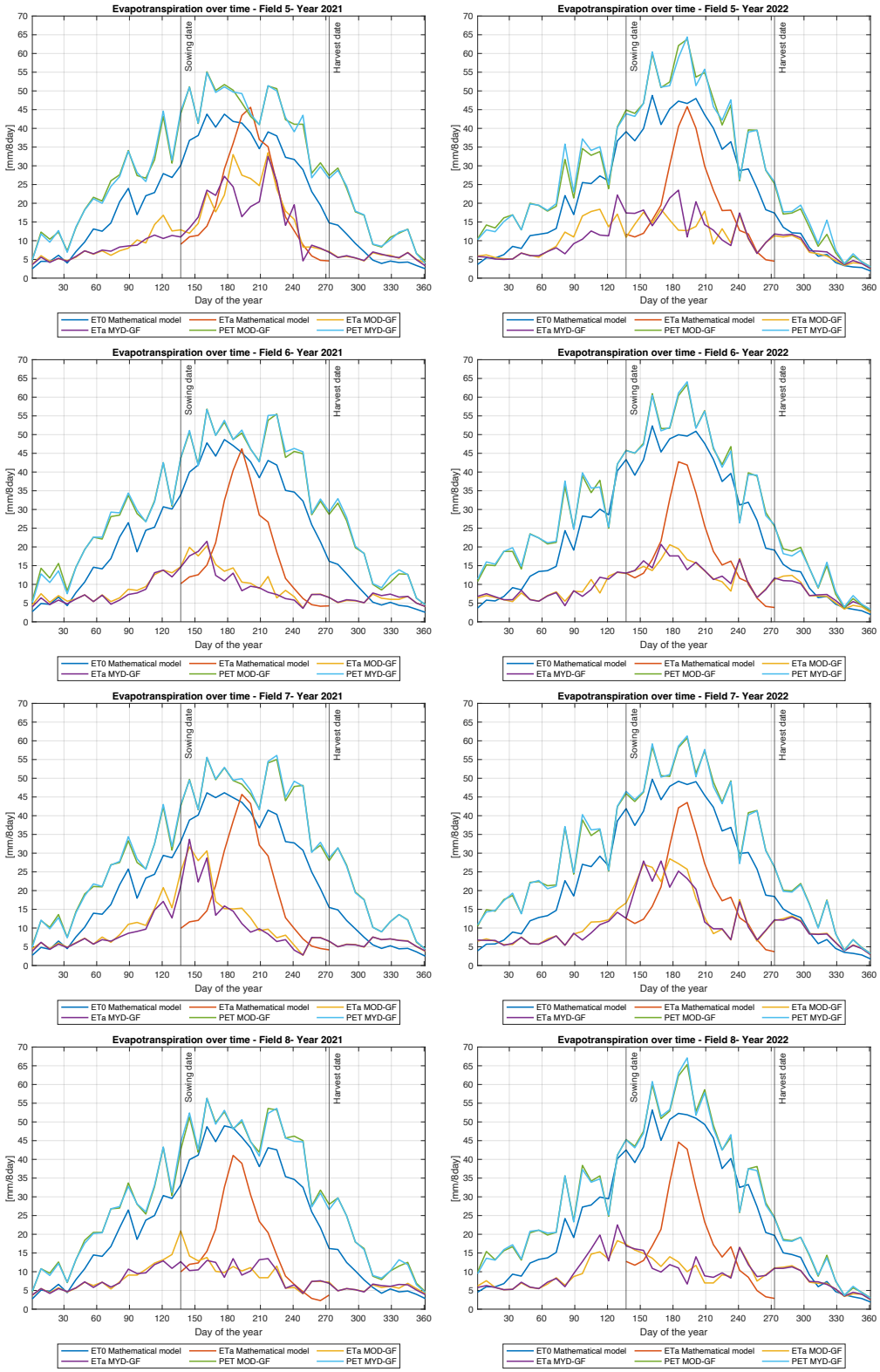
Evapotranspiration over time - Field 5- Year 2021
Evapotranspiration over time - Field 5- Year 2022
Evapotranspiration over time - Field 6- Year 2021
Evapotranspiration over time - Field 6- Year 2022
Evapotranspiration over time - Field 7- Year 2021
Evapotranspiration over time - Field 7- Year 2022
Evapotranspiration over time - Field 8- Year 2021
Evapotranspiration over time - Field 8- Year 2022
Sowing date
Harvest date
[mm/8day]
Day of the year
ET0 Mathematical model
ETa Mathematical model
ETa MOD-GF
ETa MYD-GF
PET MOD-GF
PET MYD-GF

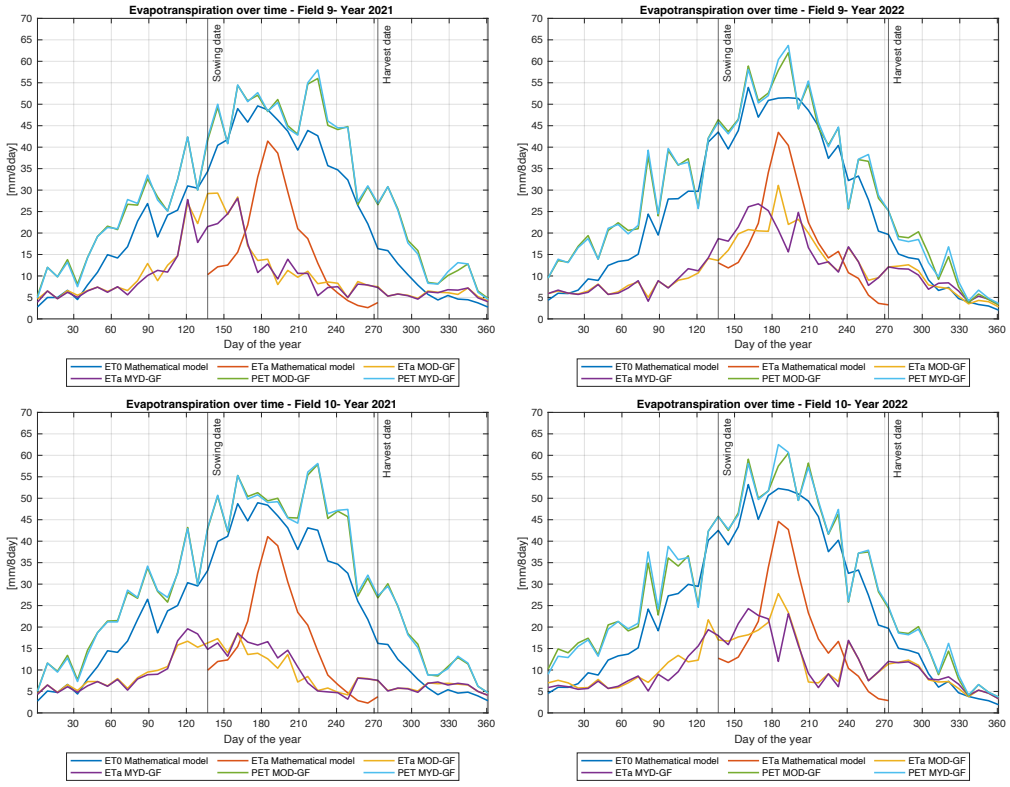

Figure 4.37: Evaporation trend of ten areas located in the province of Alessandria

From the above graphs, several observations can be made.
For all the areas considered, the trends of PET and ET_0 are similar and reflect the two previous local analyses. The values of ET_0 between 2021 and 2022 do not change significantly, while the values of PET are higher for the year 2022. This trend can be attributed to the elevated temperatures that characterized 2022, leading to a greater demand for water. Regarding evapotranspiration, there is a noticeable discrepancy between the modeled values and those acquired from satellite data for most of the areas. Notable are the values representing Fields 2, 3, 6, 8 and 10. In these areas, very low ET values have been recorded, with minimums of 5 mm/8 days. This translates into a daily evapotranspiration of less than 1 mm, which is anomalous for the considered period. Field 4 stands out as an exception where, for both years, the satellite data and the modeled data overlap. Additionally, Field 5 in the year 2021 shows a good approximation of ET levels compared to the modeled ones.
It should be noted that for the year 2021, different crops other than maize were considered and the shift of ET and PET peaks to the left is due to different sowing dates. This factor indeed influences the entire vegetative development of the plants.

4.5 Advantages and limitations

Among the advantages of the MODIS satellite product, we find the ease of estimating ET values, the availability of data almost in real-time (for the non-gap filled product), and the global coverage of the product. Indeed, the MODIS product has a significant potential for large-scale ET estimation and is readily usable. Furthermore, the data are freely available, easy to download and handle. Additionally, the MODIS product covers a time span of over twenty years, allowing for the analysis of its data over very long-time scales. This can be highly valuable in detecting climate changes for long-term comparisons.
On the other hand, this product also has some limitations. As has been observed, in some cases, the product is unable to provide a reliable estimation of ET values. Specifically, it has been observed that the MODIS product tends to underestimate ET compared to what is calculated with the soil water balance model. This underestimation can be attributed to an incorrect evaluation of soil water moisture. In fact, it is possible that the remote sensing method is not effective in cases of prolonged drought, such as in the case of 2022, as the measurement only involves the surface layer of soil and not the deeper layers. Crops in rainfed conditions are able to develop a root system that goes deeper in order to access water in the deeper and moister soil layers.
Another limitation is related to the sowing and harvesting dates. These dates depend on the type of crop, the choices made by the farmer, and the climatic conditions of that year. In this study, approximate dates were used to represent the growth period of maize and, more generally, the summer crop growth period at a regional level.
From the comparison of the results obtained with the scientific literature, it is evident that the MODIS product underestimates ET from April to October when compared with flux tower observations [33]. The underestimation of evapotranspiration by MODIS can be attributed to indirect measurements of aerodynamic resistance, canopy resistance and soil evaporation. Another study was conducted in which the algorithm was implemented to estimate these parameters more accurately by comparing them with measurements from flux towers, confirming the sensitivity of the MODIS product to these parameters [31].

Chapter 5

Conclusions

The following study was conducted to assess the MODIS satellite evapotranspiration product in order to quantify crop water stress in the Piedmont region. The MODIS satellite product has significant potential for large-scale evapotranspiration (ET) estimation, as it provides global coverage of the Earth's surface and is a ready-to-use product. The satellite approach is innovative in this context because achieving accurate ET estimates at different spatial and temporal scales can be challenging. Furthermore, it proves to be highly useful for generating time series data and monitoring long-term changes.
In order to assess the quality of the satellite product, it was compared with a mathematical soil water balance model. This model provides an estimation of crop evapotranspiration based on the Food and Agriculture Organization guidelines (FAO No. 56). The time frame of the analysis includes the two-year period 2021-2022, as these years were perceived as impacted by below-average rainfall and higher temperatures compared to seasonal averages. This condition is also confirmed in the annual reports of Arpa Piemonte, which highlighted that the high temperatures and drought of the year 2022 were unprecedented in the historical context. They characterized this year as being affected by a rare and extreme event of intense and widespread drought.
At first, a regional analysis was conducted in order to evaluate the evapotranspiration trend during the summer periods. The choice of the summer period is due to the fact that most of the summer seasonal crops are cultivated during this time. The regional analysis demonstrated a good estimation of evapotranspiration, with higher values in the flat areas and a decreasing trend in the data as altitude progressively increased. This trend is attributed to the greater extent of cultivation in the flat areas. Exceptions to this trend were observed in the plain areas around Turin and Alessandria, where values below the seasonal average were recorded. Based on these results, further local-scale analyses were conducted. To carry out these analyses, uniformly cultivated maize areas were identified in the provinces

of Turin and Alessandria.
The local analysis in the province of Turin revealed an underestimation of satellite data compared to modeled data for both areas under study and for both years, amounting to approximately 17-20 mm/8-day during the central growth phase of maize. When observing the trends of PET (Potential Evapotranspiration) and ET_0 (Reference Evapotranspiration), these two variables exhibited similar patterns, with almost complete overlap. The discrepancy between modeled and satellite-based ET values was further confirmed by the lack of correlation between them, as analyzed through scatter plots where they were compared to ET_0 and PET, respectively.
The analysis in Alessandria showed similar results for PET and ET_0 but even more pronounced discrepancies for ET, with an underestimation compared to the model of approximately 22 mm/8-day. Specifically, the evapotranspiration data are significantly below the summer averages, sometimes falling below 1 mm/day. Once again, no correlation was found between the modeled and satellite-acquired data. Among the eleven areas analyzed in the province of Alessandria, there are exceptions in two fields where there is correspondence between the satellite data and the modeling.
Previous scientific studies have demonstrated an underestimation of evapotranspiration compared to flux tower observations during the period from April to October, which corresponds to the period under analysis. It has been further shown that the underestimation of evapotranspiration by MODIS can be attributed to indirect measurements of aerodynamic resistance, canopy resistance, and soil evaporation. A scientific study was conducted in which the algorithm was implemented to estimate these parameters more accurately by comparing them with measurements from flux towers. This study confirmed the sensitivity of the MODIS product to these parameters. Future developments of this study could involve implementing the satellite algorithm to assess the parameters of aerodynamic resistance, canopy resistance and soil evaporation with even greater precision. Furthermore, monitoring ET through flux towers positioned in areas where anomalies have been recorded could prove useful in assessing actual ET. While observations from flux towers may not perfectly align with remote sensing images in terms of spatial scale, they still serve as the "ground-truth" benchmark commonly used for evaluating remote sensing-based ET products.

Bibliography

[1] Richard Allen et al. "FAO Irrigation and drainage paper No. 56". In: *Rome: Food and Agriculture Organization of the United Nations* 56 (Jan. 1998), pp. 26–40.

[2] BESS. *Breathing Earth System Simulator*. URL: https://www.environment.snu.ac.kr/.

[3] "Censimento Agricoltura 2021". In: (2021 (cit. on p. 43)).

[4] Silvia Coderoni and Francesco Pagliacci. "The impact of climate change on land productivity. A micro-level assessment for Italian farms". In: *Agricultural Systems* 205 (2023), p. 103565. ISSN: 0308-521X. DOI: https://doi.org/10.1016/j.agsy.2022.103565. URL: https://www.sciencedirect.com/science/article/pii/S0308521X22002013.

[5] Copernicus. *Corine Land Cover*. URL: https://land.copernicus.eu/pan-european/corine-land-cover/clc2018.

[6] Copernicus. *Soil Water Index*. URL: www.land.copernicus.eu.

[7] "CREA report 2020". In: *Consiglio per la ricerca in aricoltura e l'analisi dell'economia agraria* (2020).

[8] ESA. *SNAP*. URL: www.earth.esa.int/eogateway/tools/snap.

[9] EUMETSAT. *Satellite Application Facility on Land Surface Analysis*. URL: https://landsaf.ipma.pt/en/data/products/evapotranspiration-turbulent-fluxes/.

[10] FAO. *Crop information - maize*. URL: www.fao.org.

[11] GLEAM. *Global Land Evapotranspiration Amsterdam Model*. URL: www.gleam.eu.

[12] George Hargreaves and Richard Allen. "History and Evaluation of Hargreaves Evapotranspiration Equation". In: *Journal of Irrigation and Drainage Engineering-asce - J IRRIG DRAIN ENG-ASCE* 129 (Feb. 2003). DOI: 10.1061/(ASCE)0733-9437(2003)129:1(53).

[13] Samuel O. Ihuoma and Chandra A. Madramootoo. "Recent advances in crop water stress detection". In: *Computers and Electronics in Agriculture* 141 (2017), pp. 267–275. ISSN: 0168-1699. DOI: https://doi.org/10.1016/j.compag.2017.07.026. URL: https://www.sciencedirect.com/science/article/pii/S0168169916310766.

[14] IPCC. "Climate Change 2022: Impacts, Adaptation and Vulnerability. Working Group II Contribution to the Sixth Assessment Report of the Intergovernmental Panel on Climate Change." In: (2022). URL: https://www.ipcc.ch/report/sixth-assessment-r%20eport-working-group-ii/.

[15] Nader Katerji, Pasquale Campi, and Marcello Mastrorilli. "Productivity, evapotranspiration, and water use efficiency of corn and tomato crops simulated by AquaCrop under contrasting water stress conditions in the Mediterranean region". In: *Agricultural Water Management* 130 (2013), pp. 14–26. ISSN: 0378-3774. DOI: https://doi.org/10.1016/j.agwat.2013.08.005. URL: https://www.sciencedirect.com/science/article/pii/S0378377413002084.

[16] The Level-1, Atmosphere Archive, and Distribution System Distributed Active Archive Center. *ladsweb.modaps.eosdis.nasa.gov*. URL: https://ladsweb.modaps.eosdis.nasa.gov.

[17] MathWorks. *MATLAB*. URL: www.mathworks.com/products/matlab.

[18] Centro meteo. *Clima Piemonte*. URL: www.www.centrometeo.com/articoli-reportage-approfondimenti/climatologia/5408-clima-piemonte.

[19] NASA. *MODIS*. URL: www.modis.gsfc.nasa.gov.

[20] NASA. *MODIS Overview*. URL: www.lpdacc.usgs.gov.

[21] Arpa Piemonte. *Arpa Piemonte*. URL: www.arpa.piemonte.it.

[22] Arpa Piemonte. *Arpa Piemonte, Dati ambientali*. URL: https://www.arpa.piemonte.it/dati-ambientali.

[23] Arpa Piemonte. *Dataset su griglia NWIOI*. URL: www.arpa.piemonte.it/rischinaturali/tematismi/clima/confronti-storici/dati/dati.html.

[24] Regione Piemonte. *Censimento agricolo*. URL: www.regione.piemonte.it.

[25] Regione Piemonte. *Geoportale Piemonte*. URL: www.geoportale.piemonte.it.

[26] QGIS. *QGIS*. URL: www.qgis.org.

[27] Matteo Rolle, Stefania Tamea, and Pierluigi Claps. "ERA5-based global assessment of irrigation requirement and validation". In: *PLOS ONE* 16 (Apr. 2021), pp. 1–21. DOI: 10.1371/journal.pone.0250979. URL: https://doi.org/10.1371/journal.pone.0250979.

[28] ISMEA- Istituto di Servizi per il Mercato Agricolo Alimentare. "Standardizzazione delle procedure per la valutazione dei danni alle colture vegetali – Mais da granella". In: (June 2021).

[29] National Snow and Ice Data Center. *nsidc.org*. URL: https://nsidc.org/sites/default/files/modis-terra-v-aqua.pdf.

[30] "User's Guide MODIS Global Terrestrial Evapotranspiration (ET) Product (MOD16A2/A3 and Year-end Gap-filled MOD16A2GF/A3GF) NASA Earth Observing System MODIS Land Algorithm (For Collection 6.1)". In: (2021).

[31] Kun Zhang et al. "Parameter Analysis and Estimates for the MODIS Evapotranspiration Algorithm and Multiscale Verification". In: *Water Resources Research* 55.3 (), pp. 2211–2231. DOI: https://doi.org/10.1029/2018WR023485. eprint: https://agupubs.onlinelibrary.wiley.com/doi/pdf/10.1029/2018WR023485. URL: https://agupubs.onlinelibrary.wiley.com/doi/abs/10.1029/2018WR023485.

[32] Chaolei Zheng, Li Jia, and Guangcheng Hu. "Global land surface evapotranspiration monitoring by ETMonitor model driven by multi-source satellite earth observations". In: *Journal of Hydrology* 613 (2022), p. 128444. ISSN: 0022-1694. DOI: https://doi.org/10.1016/j.jhydrol.2022.128444. URL: https://www.sciencedirect.com/science/article/pii/S0022169422010149.

[33] Wenbin Zhu et al. "Multi-scale evaluation of global evapotranspiration products derived from remote sensing images: Accuracy and uncertainty". In: *Journal of Hydrology* 611 (2022), p. 127982. ISSN: 0022-1694. DOI: https://doi.org/10.1016/j.jhydrol.2022.127982. URL: https://www.sciencedirect.com/science/article/pii/S0022169422005571.